

# Statistical characterization of erosion and sediment transport mechanics in shallow tidal environments. Part 2: suspended sediment dynamics

Davide Tognin<sup>1,2</sup>, Andrea D'Alpaos<sup>2</sup>, Luigi D'Alpaos<sup>1</sup>, Andrea Rinaldo<sup>1,3</sup>, and Luca Carniello<sup>1</sup>

<sup>1</sup>Department of Civil, Environmental, and Architectural Engineering, University of Padova, Padova, Italy

<sup>2</sup>Department of Geosciences, University of Padova, Padova, Italy

<sup>3</sup>Laboratory of Ecohydrology ECHO/IEE/ENAC, École Polytechnique Fédérale de Lausanne, Lausanne, Switzerland

**Correspondence:** Davide Tognin (davide.tognin@unipd.it)

**Abstract.** A proper understanding of sediment transport dynamics, critically including resuspension and deposition processes of suspended sediments, is key to the morphodynamics of shallow tidal environments. Aiming to account for deposition mechanics in a synthetic theoretical framework introduced to model erosion dynamics (D'Alpaos et al., Companion paper), here we investigated suspended sediment dynamics. A complete spatial and temporal coverage of suspended sediment concentration (SSC) required to effectively characterize resuspension events is hardly available through observation alone, even combining point measurements and satellite images, but it can be retrieved by properly calibrated and tested numerical models. We analyzed one-year-long time series of SSC computed by a bi-dimensional, finite-element model in six historical configurations of the Venice Lagoon in the last four centuries. Following the peak-over-threshold theory, we statistically characterized suspended sediment dynamics by analyzing interarrival times, intensities and durations of over-threshold SSC events. Our results confirm that, as for erosion events, SSC can be modeled as a marked Poisson process in the intertidal flats for all the considered historical configurations of the Venice Lagoon because exponentially distributed random variables well describe interarrival times, intensity and duration of over-threshold events. Moreover, interarrival times, intensity and duration describing local erosion and over-threshold SSC events are highly related, although not identical because of the non-local dynamics of suspended sediment transport related to advection and dispersion processes. Owing to this statistical characterization of SSC events, it is possible to generate synthetic, yet realistic, time series of SSC for the long-term modeling of shallow tidal environments.

## 1 Introduction

Suspended sediment dynamics in shallow tidal systems play a significant role as they influence geomorphic and ecological processes, that ultimately determine the long-term morphodynamic evolution of coastal, estuarine and lagoonal landscapes (Woodroffe, 2002; Masselink et al., 2014). Physical processes that drive sediment resuspension and transport in tidal environments are influenced by different hydrodynamic and sedimentological factors over a wide range of spatial and temporal scales.

Both tide and waves represent key drivers controlling sediment entrainment and transport in shallow tidal environments (Wang, 2012). The tide rise and fall generate currents that propagate along the preferential pathways provided by the channel network (Hughes, 2012) but, as the tide overflows on the adjoining intertidal flats, it is strongly affected by shallower water and friction effects (Friedrichs and Madsen, 1992), so that its velocity and, hence, its resuspension capacity can diminish considerably. Whereas, wind waves with a typically short period can generate wave-orbital motions capable of resuspending intertidal-flat sediments (Anderson, 1972; Dyer et al., 2000; Carniello et al., 2005; Green, 2011). Therefore, stochastic wave-forced resuspension can increase locally, mainly under storm conditions, and can overcome the cyclic resuspension by tidal currents in generating high turbidity (Green et al., 1997; Ralston and Stacey, 2007; Sanford, 1994). Wave-driven resuspension and erosion together with tide- and wave-driven sediment transport give rise to mechanisms leading to basin-wide sediment movement, which strongly shape the morphology of shallow tidal systems (e.g., Nichols and Boon, 1994; Green and Coco, 2007; Carniello et al., 2011; Green and Coco, 2014). The repeated cycles of erosion, resuspension and deposition, that sediments may undergo, winnow fine particles from coarser ones and, thus, modify sediment distribution and textural properties of intertidal flats and subtidal platforms, influencing physical and biological processes (Dyer, 1989), light climate (Moore and Wetzel, 2000) and ecosystem productivity (Carr et al., 2010; Lawson et al., 2007; Carr et al., 2016; McSweeney et al., 2017).

Moreover, resuspension dynamics are mutually linked to numerous biological and ecological processes (Temmerman et al., 2007; Kirwan and Murray, 2007; D'Alpaos et al., 2007, 2011; Marani et al., 2013). Benthic vegetation and algae play a key role in increasing sediment stability of subtidal platforms (Nepf, 1999; Tambroni et al., 2016; Venier et al., 2014). In fact, the interaction of flexible vegetation and bedforms can reduce the effective bed shear stress and, consequently, sediment mobility. Similarly, the action of halophytic vegetation over salt marshes has a significant impact on landscape development, enhancing accretion, both by directly trapping inorganic sediment and by producing organic matter (Marani et al., 2013; D'Alpaos and Marani, 2016; Roner et al., 2016). However, some studies have also suggested that, although vegetation anchors sediment through rooting and by slowing water flows, erosion and scour of the proximal sediments can also be enhanced (Temmerman et al., 2007; Tinoco and Coco, 2016). Microalgae, although small, may also heavily impact sediment erodibility. Indeed, extracellular polymeric secretions (EPS) of microphytobenthos can increase grain adhesion and consequently erosion threshold of the sedimentary substrate (Le Hir et al., 2007; Parsons et al., 2016; Chen et al., 2019). As a result, sediment resuspension decreases in the presence of EPS, which affects light availability and, in turn, microalgae proliferation, thus triggering positive feedback (Pivato et al., 2019). Benthic fauna can further modify the bed sediment by changing its geotechnical properties and erosion resistance (Widdows and Brinsley, 2002; Vu et al., 2017).

Owing to the complexity of the underlying processes and the interplay between physical and biological drivers, sediment dynamics in shallow tidal systems are rather entangled. Therefore, observation-based approaches have been widely adopted to investigate the suspended sediment concentration (hereafter SSC), using either in situ point measurements (e.g., Wren et al., 2000; Gartner, 2004; Brand et al., 2020) or remote sensing and satellite image analysis (Miller and McKee, 2004; Ruhl et al., 2001; Volpe et al., 2011). However, both these techniques have some drawbacks. In situ measurements can provide an accurate description of the temporal dynamics of SSC, but lacks information on its spatial heterogeneity. Moreover, acoustic and optical sensors installed in point turbidity stations require periodic cleaning to prevent failure due to biofouling. Whereas, satellite-

based data can supply instantaneous information on SSC spatial variability, but are barely informative on its temporal dynamics. Indeed, SSC events can hardly be fully captured by satellites with fixed and often long revisit periods. Furthermore, intense SSC typically occurs during severe storms, frequently characterized by clouds, which make satellite data useless. As a matter of fact, reliable long-term SSC time series at the basin scale, required for the statistical analysis performed herein, are seldom available.

In order to overcome these shortcomings and to exploit measurements of in situ point observations and satellite images, these data can be combined to calibrate and test numerical models (Ouillon et al., 2004; Carniello et al., 2014; Maciel et al., 2021), thereby, using them as physically-based “interpolators” to compute temporal and spatial SSC dynamics. However, computing SSC dynamics over time scales of centuries in order to model the morphodynamic evolution of tidal environments through fully-fledged numerical models is rather difficult owing to the computational burden involved. Therefore, modeling the long-term evolution of tidal systems requires comprehending the physics of the processes in order to properly characterize them in the framework of simplified approaches (Murray, 2007).

Pointing to the development of a synthetic theoretical framework to represent intense SSC events and to account for their landscape-forming action on tidal basin morphology, we applied a two-dimensional finite element model to simulate the interaction among wind waves, tidal current and sediment transport in several historical configurations of the Venice Lagoon. In particular, we used a previously-calibrated and widely-tested Wind Wave-Tidal Model (WWTM) (Carniello et al., 2005, 2011) coupled with a sediment transport model (Carniello et al., 2012) to investigate hydrodynamics and suspended sediment dynamics in the following six historical configurations of the Venice Lagoon: 1611, 1810, 1901, 1932, 1970, and 2012. For each of them, we run a one-year-long simulation forced with representative tidal and meteorological boundary conditions. The computed SSC time series have been analyzed on the basis of the peak-over-threshold (POT) theory, following the approach introduced by D’Alpaos et al. (2013) and expanding the analysis performed by Carniello et al. (2016) to study the statistics of SSC in the present configuration of the Venice Lagoon.

This study aims to expand this analysis to other historical configurations of the Venice Lagoon (Figure 1) in order to unravel the effects on sediment transport of the morphological and anthropogenic modifications experienced by the lagoon in the last four centuries and to test whether SSC dynamics can be modeled as a marked Poisson process also when accounting for the morphological evolution of the basin. The latter represents an interesting goal, being the use of stochastic frameworks particularly promising for long-term studies, as pointed out by their increasing popularity in hydrology and geomorphology to describe the long-term behaviour of geophysical processes (e.g., Rodriguez-Iturbe et al., 1987; D’Odorico and Fagherazzi, 2003; Botter et al., 2013; Park et al., 2014; Bertassello et al., 2018). Nonetheless, applications to tidal systems are still quite uncommon (D’Alpaos et al., 2013; Carniello et al., 2016). Our analysis provides a spatial and temporal characterization of resuspension events for the Venice Lagoon from the beginning of the seventeenth century to the present, in order to show how morphological modification affected sediment transport and to set a stochastic framework to forecast future scenarios.

## 2 Materials and Methods

90 The Venice Lagoon (Figure 1) underwent different morphological changes over the last four centuries, in particular due to anthropogenic modifications (D’Alpaos, 2010; Finotello et al., 2022). From the beginning of the fifteenth century, the main rivers (Brenta, Piave, and Sile) were gradually diverted in order to flow directly into the sea and prevent the lagoon from silting up, but this triggered a sediment starvation condition. Later, during the last century, the inlets were provided with jetties and deep navigation channels were excavated to connect the inner harbour with the sea (D’Alpaos, 2010; Sarretta et al., 2010).

95 The jetties deeply changed the hydrodynamics at the inlets establishing an asymmetric hydrodynamic behaviour responsible for a net export of sediment toward the sea (Martini et al., 2004; Finotello et al., 2022), especially during severe storm events, which are responsible for the resuspension of large sediment volumes (Carniello et al., 2012). In general, these modifications heavily influenced sediment transport triggering strong erosion processes that were further aggravated by sea-level rise. The net sediment loss clearly emerges from the comparison among the different surveys of the Venice Lagoon, which show a

100 generalized deepening of tidal flats and subtidal platforms as well as a reduction of salt-marsh area (Carniello et al., 2009). Indeed, in the last century, the average tidal-flat bottom elevation lowered from -0.51 m to -1.49 m above mean sea level (a.m.s.l.), while the salt-marsh area progressively shrank from 164.36 km<sup>2</sup> to 42.99 km<sup>2</sup> (Tommasini et al., 2019). Moreover, repeated closures of storm-surge barriers designed to protect the city of Venice from flooding and known as Mo.S.E. system are expected to further exacerbate this morphological degradation by cutting off significant supplies of inorganic sediments

105 brought in by intense storm-surge events (Tognin et al., 2022).

To study the influence of these morphological changes on suspended sediment dynamics, we considered six different historical configurations of the Venice Lagoon, ranging from the beginning of the seventeenth century to today (Figure S1). The three most ancient configurations (i.e. 1611, 1810, and 1901) were modeled by relying on historical maps, whereas the topographic surveys carried out by the Venice Water Authority (Magistrato alle Acque di Venezia) in 1932, 1970, and 2003 were used for

110 the more recent ones (D’Alpaos, 2010; Finotello et al., 2022). Due to some morphological modifications at the three inlets associated with the Mo.S.E. system and almost completed in 2012, the 2003 configuration was updated, so we will refer to this configuration as the 2012 configuration. For a detailed description of the methodology applied for the reconstruction of the historical configurations of the Venice Lagoon and additional information on the more recent bathymetric data, we refer the reader to Tommasini et al. (2019). Further details on the geomorphological setting and the implications on erosion and

115 resuspension events are reported in D’Alpaos et al. (Companion paper).

### 2.1 Numerical Model

The flow field and sediment transport in the six configurations of the Venice Lagoon are computed by using a numerical model, consisting of three modules. The coupling of the hydrodynamic module with the wind-wave module (WWTM) describes the hydrodynamic flow field together with the generation and propagation of wind waves (Carniello et al., 2005, 2011), while

120 the sediment transport and the bed evolution module (STABEM) evaluates the sediment dynamics and the effects on the morphology (Carniello et al., 2012). All modules share the same computational grid.



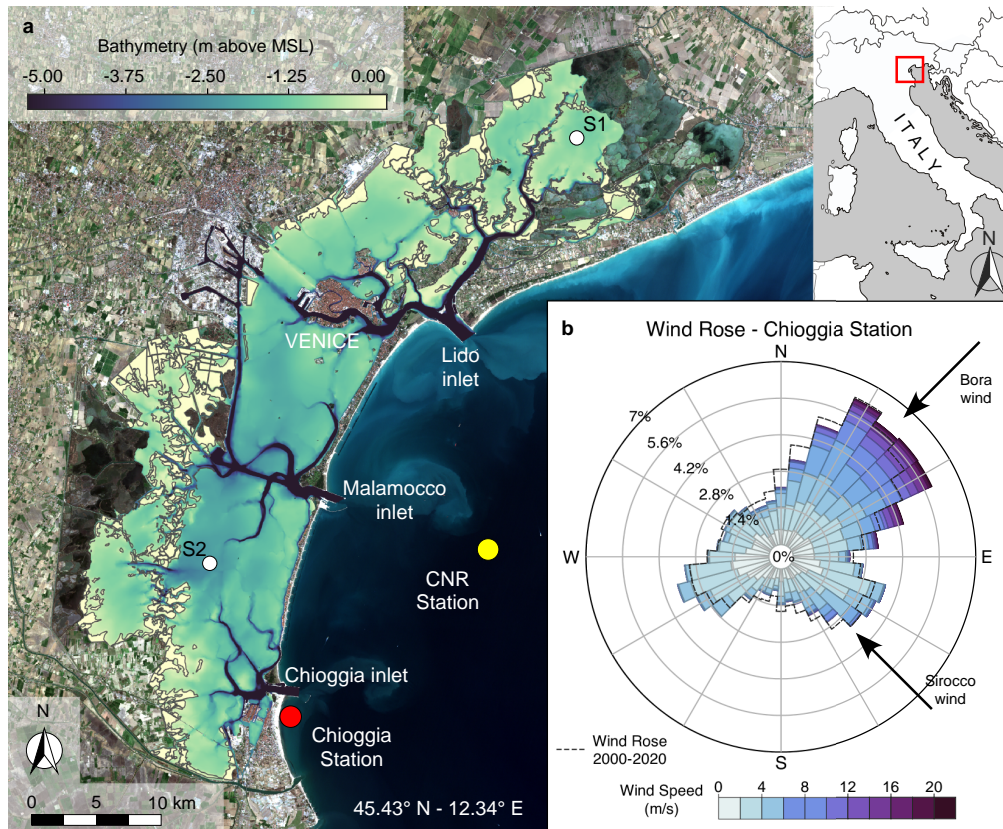


**Figure 1. Morphological features and wind conditions characterizing the Venice Lagoon.** **a**, Bathymetry of the Venice Lagoon (Base satellite image: Copernicus Sentinel data 2020, <https://scihub.copernicus.eu/>). The locations of the anemometric (Chioggia) and oceanographic (CNR Oceanographic Platform) stations are also shown, together with the locations of the two stations (S1 and S2) for which we provide detailed statistical characterization of over-threshold events. **b**, Wind rose for the data recorded at the Chioggia station in 2005. Dashed line shows the wind rose for the period 2000-2020.

The hydrodynamic module solves the 2-D shallow water equations using a semi-implicit staggered finite element method based on Galerkin's approach (Defina, 2000; Martini et al., 2004). The equations are suitably rewritten in order to deal with flooding and drying processes in morphologically irregular domains. The Strickler equation is used to evaluate the bottom shear stress induced by currents,  $\tau_c$ , considering the case of turbulent flow over a rough wall. Further, the hydrodynamic module provides the flow field characteristic requested by the wind-wave module to simulate the generation and propagation of wind waves.

The wind-wave module (Carniello et al., 2011) solves the wave action conservation equation parametrized using the zero-order moment of the wave action spectrum in the frequency domain (Holthuijsen et al., 1989). The peak wave period is related to the local wind speed and water depth, and this empirical correlation function is used to determine the spatial and temporal distribution of the wave period (Breugem and Holthuijsen, 2007; Carniello et al., 2011; Young and Verhagen, 1996). The

bottom shear stress induced by wind waves,  $\tau_{ww}$ , is computed as a function of the maximum horizontal orbital velocity at the bottom, which is related to the significant wave height through the linear theory. Owing to the non-linear interaction between the wave and current boundary layers, the maximum bottom shear stress,  $\tau_{wc}$ , is enhanced beyond the linear addition of the wave-alone and current-alone stresses: in the WWTM this is considered adopting the empirical formulation suggested by Soulsby (1995, 1997).

The sediment transport and bed evolution module (STABEM) is based on the solution of the advection-diffusion equation and Exner's equation (Carniello et al., 2012). This module uses two size classes of sediments to describe the bed composition (i.e. non-cohesive sand and cohesive mud), in order to consider the simultaneous presence of cohesive and non-cohesive sediment typically characterizing tidal lagoons (van Ledden et al., 2004). The local mud content, which varies both in space and time, marks off the transition between the cohesive and non-cohesive behaviour of a mixture, and, consequently, determines the critical value for bottom shear stress, which is locally estimated based on the critical values assumed for pure sand and pure mud. However, this task is tough and site-specific, and, moreover, field data are often limited compared to the spatial variability of bed composition. To address this issue, field surveys in the Venice Lagoon have been used to identify an empirical relationship between the local bed composition and both the local bottom elevation and the distance from the inlets. We refer to Carniello et al. (2012) for further details.

Another peculiarity of the sediment transport module is the stochastic approach chosen to model the near-threshold conditions for sediment entrainment. Indeed, in shallow tidal basins, resuspension events are periodically driven by bottom shear stresses that slightly exceed the erosion threshold. The bottom shear stress, as well as the critical shear stress, is very unsteady owing to the non-uniform flow velocity, wave characteristics and small-scale bottom heterogeneity. Hence, following the stochastic approach suggested by Grass (1970), both the total bottom shear stress,  $\tau_{wc}$ , and the critical shear stress for erosion,  $\tau_c$ , are treated as random variables ( $\tau'_{wc}$ , and  $\tau'_c$ , respectively) with lognormal distributions, and their expected values are those calculated by WWTM and STABEM. Consequently, the erosion rate depends on the probability that  $\tau_{wc}$ , exceeds  $\tau'_c$  (Carniello et al., 2012).

These coupled numerical models were used to perform one-year-long simulations within the six different computational grids representing the historical configuration of the Venice Lagoon and the portion of the Adriatic Sea in front of it. Hourly tidal level gauged at the Consiglio Nazionale delle Ricerche (CNR) Oceanographic Platform, located in the Adriatic Sea offshore of the lagoon, and wind velocities and directions recorded at the Chioggia anemometric station are imposed as boundary conditions (Figure 1).

All configurations were forced with tidal levels and wind climate measured during the whole year 2005, as this year was selected as a representative year, being the probability distribution of wind speed at the Chioggia Station in 2005 the closest to the mean annual probability distribution in the period 2000-2020 (Figure 1). Forcing all the historical configurations of the Venice Lagoon with the same wind and tidal conditions enables us to isolate the effects of the morphological modifications on the wind-wave field, hydrodynamics and sediment dynamics.

Another important issue to consider when studying SSC dynamics in shallow tidal environments is the presence of benthic and halophytic vegetation, which both shelters the bed against the hydrodynamic action and increases the local critical shear

stress for erosion because of the presence of roots. While the presence of halophytic vegetation over salt marshes is almost ubiquitous, reconstructing the presence of benthic vegetation on the tidal flats is much more difficult even for the present configuration of the lagoon and practically impossible for the ancient configurations (Goodwin et al., 2023). For the above reasons and for the sake of homogeneity, the simulations of the present study neglect the presence of benthic vegetation on the tidal flat and assume all salt-marsh platforms to be completely vegetated in each configuration of the lagoon, thus neglecting sediment resuspension over them (Christiansen et al., 2000; Temmerman et al., 2005).

## 2.2 Peak Over Threshold Analysis of SSC

Sediment transport dynamics in tidal environments are the results of the complex interplay between hydrodynamic, biologic, and geomorphologic processes. This interplay between different factors can be fully framed only by taking into account both its deterministic and stochastic components. As an example, Carniello et al. (2011) argued that morphological dynamics in the Venice Lagoon are mostly linked to a few severe resuspension events induced by wind waves, whose dynamics are markedly stochastic in the present configurations (D'Alpaos et al., 2013; Carniello et al., 2016). Measurements confirm that high SSC events are also important sediment suppliers for salt marshes (Tognin et al., 2021).

In the present work, we used the peak-over-threshold theory (POT) (Balkema and de Haan, 1974) to analyze temporal and spatial dynamics of the total SSC at any location within each selected configuration of the Venice lagoon. First, a minimum-intensity threshold,  $C_0$ , was chosen to identify the set of over-threshold events from the modeled SSC record, and then a statistical analysis of interarrival times, durations and intensities of the exceedances of the threshold was carried out. The interarrival time is defined as the time interval between two consecutive upcrossings of the threshold, the duration of the events is the time elapsed between any upcrossing and the subsequent downcrossing of the threshold, and, finally, the intensity is calculated as the largest exceedance of the threshold in the time-lapse between an upcrossing and the subsequent downcrossing. These three variables are characterized by means of their probability density functions and the corresponding moments for any location in all the considered configurations of the Venice Lagoon, in order to provide a complete description of the SSC pattern. The nature of the stochastic processes can be determined by the analysis of the interarrival times distribution. Indeed, resuspension events can be mathematically modeled as a marked Poisson process if the interarrival times between subsequent exceedances of the threshold,  $C_0$ , are independent and exponentially distributed random variables. In order to assess that over-threshold SSC events can be modeled as a Poisson process, we performed the Kolmogorov-Smirnov (KS) goodness of fit test on the distribution of the interarrival times. In our case, the sequence of random events that define a 1-D Poisson process along the time axis is associated with a vector of random marks that defines the duration and intensity of each over-threshold event. Memorylessness is one of the most interesting features of Poisson processes because it states that the number of events observed in disjoint subperiods is an independent, Poisson-distributed random variable. According to the extreme value theory, a Poisson process emerges from a stochastic signal whenever enough high censoring threshold is chosen (Cramér and Leadbetter, 1967). However, as this present analysis is designed to remove only the weak resuspension events induced by periodic tidal currents, the critical threshold is well below the maximum observed values. As a consequence, the aim of the proposed analysis is to characterize the bulk effect of morphologically meaningful SSC events, rather than to describe the extreme events.

Notwithstanding the increasing popularity of Poisson processes for the analytical modeling of the long-term evolution of geophysical processes controlled by stochastic drivers in hydrological and geomorphological sciences (e.g., Rodriguez-Iturbe et al., 1987; D’Odorico and Fagherazzi, 2003; Botter et al., 2013; Park et al., 2014; Bertassello et al., 2018), only in the last few years this approach has been adopted for tidal systems (D’Alpaos et al., 2013; Carniello et al., 2016) and the applications  
 205 portray an encouraging framework.

### 3 Results and Discussion

The statistical characterization of suspended sediment dynamics is provided through the analysis of the one-year-long time series of the computed SSC on the basis of the POT method. The choice of the threshold value,  $C_0$ , that identifies morphologically significant over-threshold SSC events has to consider two opposite requirements. On the one hand, stochastic sediment  
 210 concentration generated by storm-induced wind waves can be distinguished from tide-modulated daily concentration only if  $C_0$  is large enough. On the other hand, too high values of  $C_0$  can lead to a non-informative analysis because of the large number of events unaccounted for. In the following, we used a constant threshold,  $C_0$ , equal to  $40 \text{ mg l}^{-1}$ , as suggested by Carniello et al. (2016) by analyzing available in-situ SSC time series and performing a sensitivity analysis for the statistical analysis of SSC events in the present configuration of the Venice Lagoon.

215 As a first step, the SSC time series provided by the numerical simulations were low-pass filtered by applying a moving average procedure with a time window of 6 hours, in order to preserve the tide-induced modulation of the signal but, at the same time, to remove artificial upcrossing and downcrossing of the threshold, generated by short-term fluctuations.

The distributions of interarrival times, intensity of peak excess and durations obtained using the POT analysis are then compared with an exponential distribution performing the KS test with a significance level  $\alpha = 0.05$ . The KS test is replicated  
 220 at each node of the computational grids reproducing the selected configurations and the results are shown in Figure 2, where we can identify three different situations:

1. SSC events cannot be described as a Poisson process, i.e. the KS test is not satisfied for interarrival times, in the dark blue areas;
2. SSC events are indeed a marked Poisson process because interarrival times, peak excesses and durations satisfy the KS  
 225 test, and, thus, are exponentially distributed random variables, in the red areas;
3. SSC events still are a marked Poisson process but at least one between intensity and duration does not satisfy the KS test, i.e. although interarrival times follow an exponential distribution, at least one between intensity and duration does not, in the yellow areas.

The spatial distribution of mean interarrival times (Figure 3), mean intensities of peak excesses (Figure 4), and mean dura-  
 230 tions (Figure 5) of over-threshold events are shown at any location within each of the six historical configurations where SSC events can be modeled as a Poisson process (i.e., the KS test is verified for interarrival times at significance level  $\alpha = 0.05$ ).

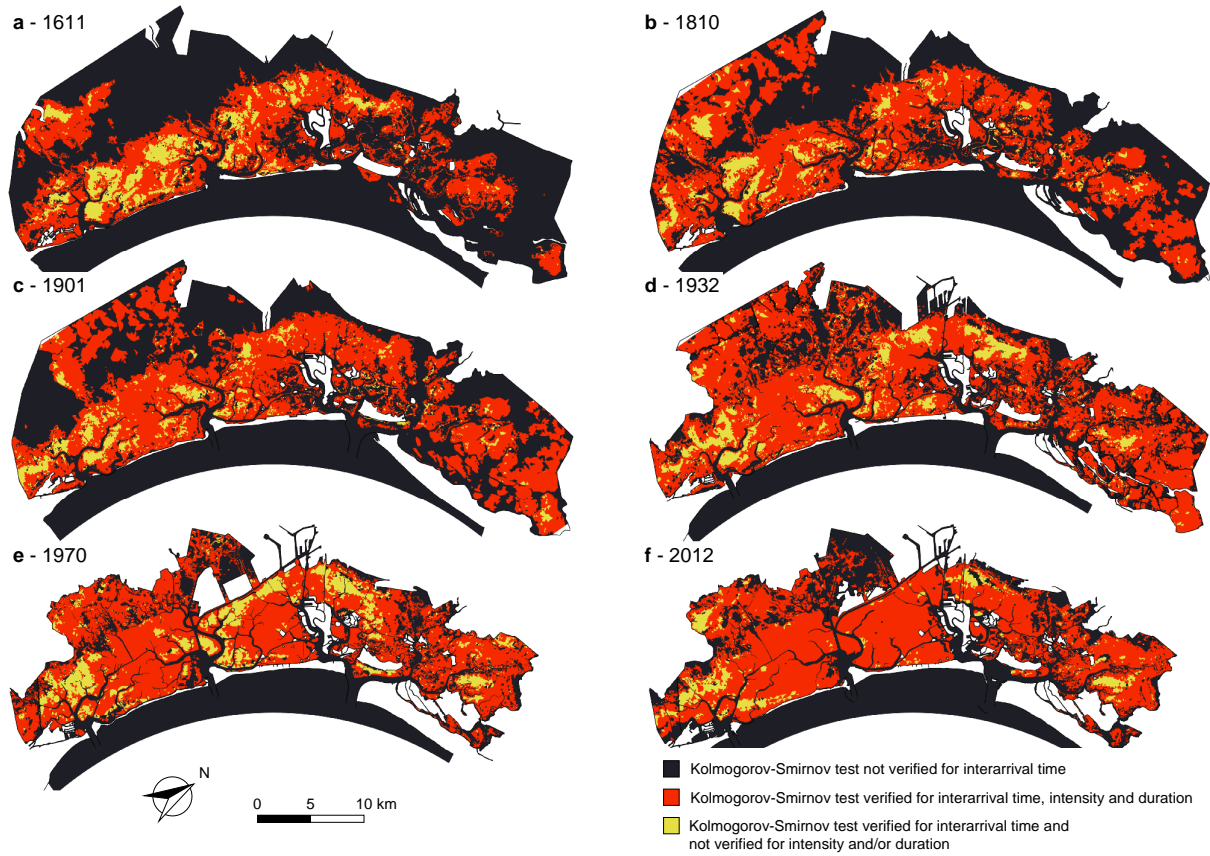


**Figure 2. Kolmogorov-Smirnov test for over-threshold SSC events.** Spatial distribution of Kolmogorov-Smirnov (KS) test at significance level ( $\alpha = 0.05$ ) for the six different configurations of the Venice Lagoon: 1611 (a), 1810 (b), 1901 (c), 1932 (d), 1970 (e), and 2012 (f). In the maps we can distinguish areas where the KS test is: not verified (dark blue); verified for all the considered stochastic variables (interarrival time, intensity over the threshold and duration) (red); verified for the interarrival time and not for intensity and/or duration (yellow).

The area of the lagoon where over-thresholds SSC events cannot be modeled as Poisson processes are mostly represented by salt marshes and tidal channels in all configurations (see dark blue areas in Figure 2), similarly to the results for erosion events (BSS) (D'Alpaos et al., Companion paper). On salt-marsh areas, both BSS and SSC thresholds ( $\tau_C$  and  $C_0$  respectively) are seldom exceeded (Figure S2 and S3), because the reduced water depth over the marsh prevents the propagation of large wind waves and the presence of halophytic vegetation limits sediment advection by promoting deposition and stabilizes the bottom preventing erosion (e.g., Möller et al., 1999; Temmerman et al., 2005; Carniello et al., 2005). Within the main tidal channels and at the three inlets, as happens for BSS, SSC dynamics are not Poissonian, but the reason why interarrival times of erosion and SSC events are not exponentially distributed are slightly different. In the main channel network and at the inlets, SSC exceeds the threshold value,  $C_0$ , very few times or it does not exceed the threshold at all, due to vertical dispersion mechanisms that decrease the local concentration of sediment in suspension in deeper areas (Figure S3). Conversely, BSS typically exceeds



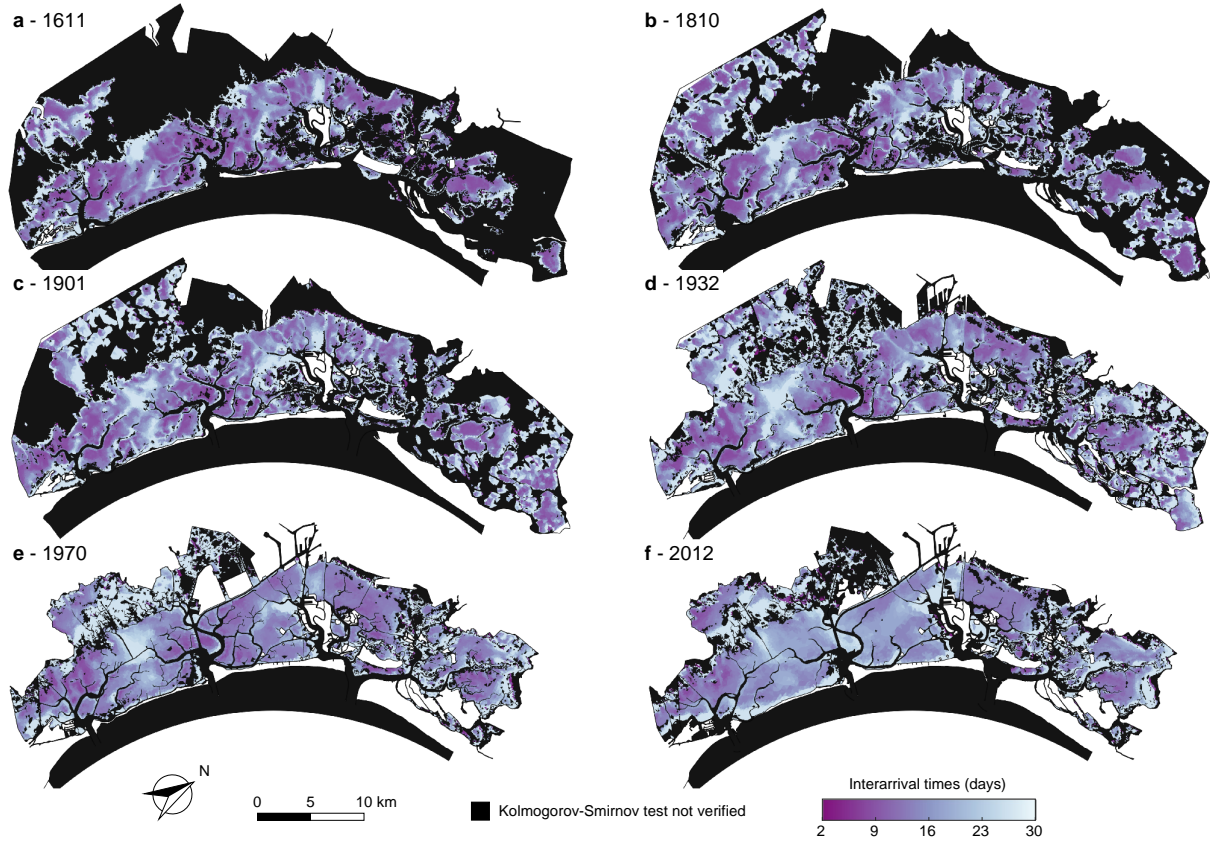


**Figure 3. Mean interarrival time of over-threshold SSC events.** Spatial distribution of mean interarrival times of over-threshold exceedances at sites where SSC events can be modeled as a marked Poisson process, as confirmed by the KS test ( $\alpha = 0.05$ ) for the six different configurations of the Venice Lagoon: 1611 (a), 1810 (b), 1901 (c), 1932 (d), 1970 (e), and 2012 (f).

the threshold  $\tau_c$  twice or four times a day (Figure S2) mainly because of the tide action but the BSS time evolution cannot be modeled as a Poisson process as confirmed by the KS test on interarrival times of over-threshold BSS events (D'Alpaos et al., Companion paper).

245 However, SSC events can be modeled as a Poisson process over wide areas of the six configurations of the Venice Lagoon, in particular over tidal flats and subtidal platforms (see red and yellow areas in Figure 2). As a consequence, SSC dynamics can be effectively modeled by using a synthetic framework based on Poisson processes over widespread portions of the different morphological configurations experienced by the Venice Lagoon in the last four centuries.

Large interarrival times (i.e., larger than 30 days, Figure 3) are observed on tidal flats close to the main channel network  
 250 because dilution processes within higher water depth, enhanced by the higher velocities in these sites, reduce sediment concentration, and hence only severe, but infrequent, events can lead to an exceedance of the threshold. Sheltered areas are also characterized by large interarrival times as represented by the northern portion of the lagoon, which is protected by the main-

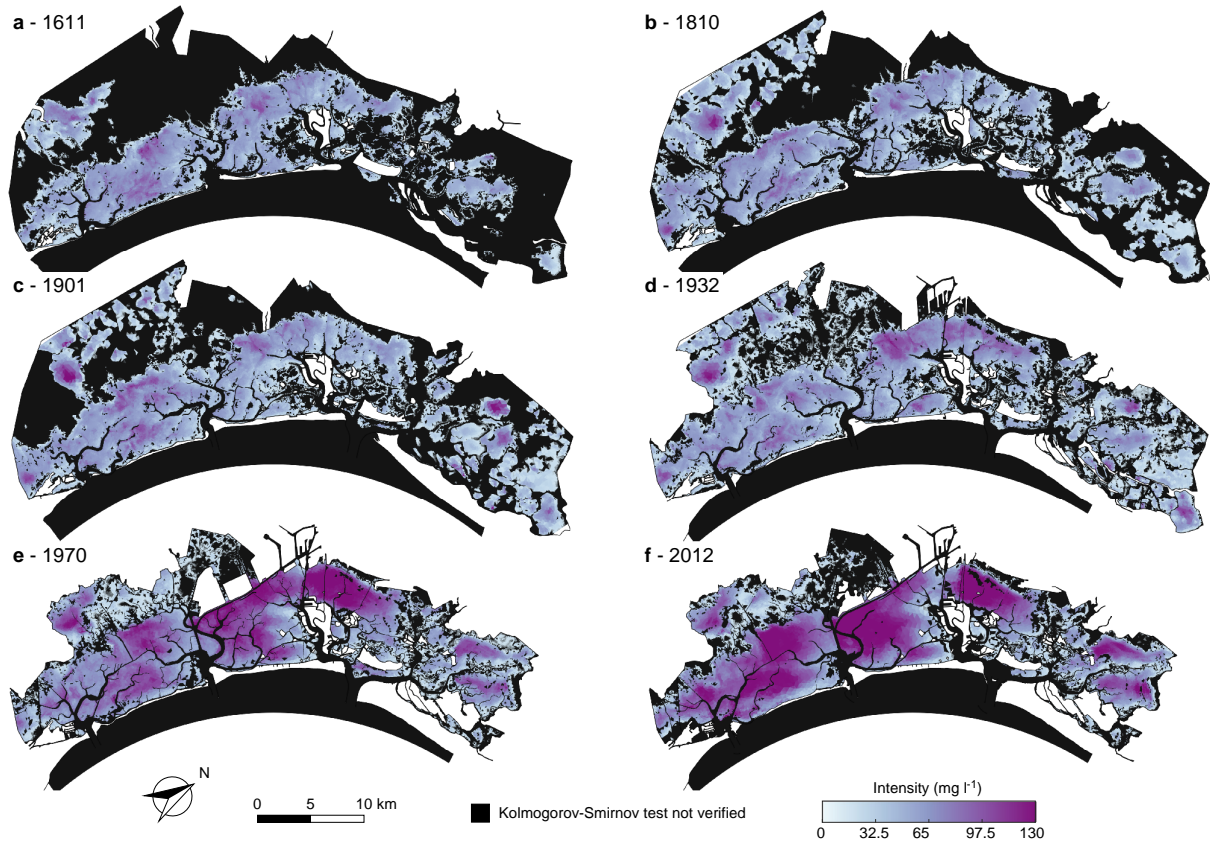


**Figure 4. Mean intensity of over-threshold SSC events.** Spatial distribution of mean intensity of peak excesses of over-threshold exceedances at sites where SSC events can be modeled as a marked Poisson process, as confirmed by the KS test ( $\alpha = 0.05$ ) for the six different configurations of the Venice Lagoon: 1611 (a), 1810 (b), 1901 (c), 1932 (d), 1970 (e), and 2012 (f).

land from the north-easterly Bora wind, which is the most intense and morphologically significant wind in the Venice Lagoon (Figure 1b), and where the presence of extensive salt-marsh areas continuously interrupts the propagation of wind waves. In this case, the reduced number of upcrossing events, and, consequently, large interarrival times is due to the sheltering action of salt marshes and islands in reducing wind-wave resuspension. SSC events over the marsh platform slightly changed through centuries. In the three oldest configurations (i.e., 1611, 1810 and 1901) mainly because of the wide extent of salt marshes, resuspension events over salt marshes do not even reach the threshold, as shown by the number of upcrossing (Figure S3). In the more recent ones, where salt-marsh extent importantly decreases, marshes start experiencing some over-threshold SSC events because of the advection of sediment from the adjacent areas, but the lower number of upcrossing allows the mean interarrival time to assume large values.

Over wide tidal flat areas, where the threshold is exceeded in all the considered configurations, the mean interarrival time generally slightly increases through the centuries (Figure S5a). This trend is more evident in the central and southern parts of

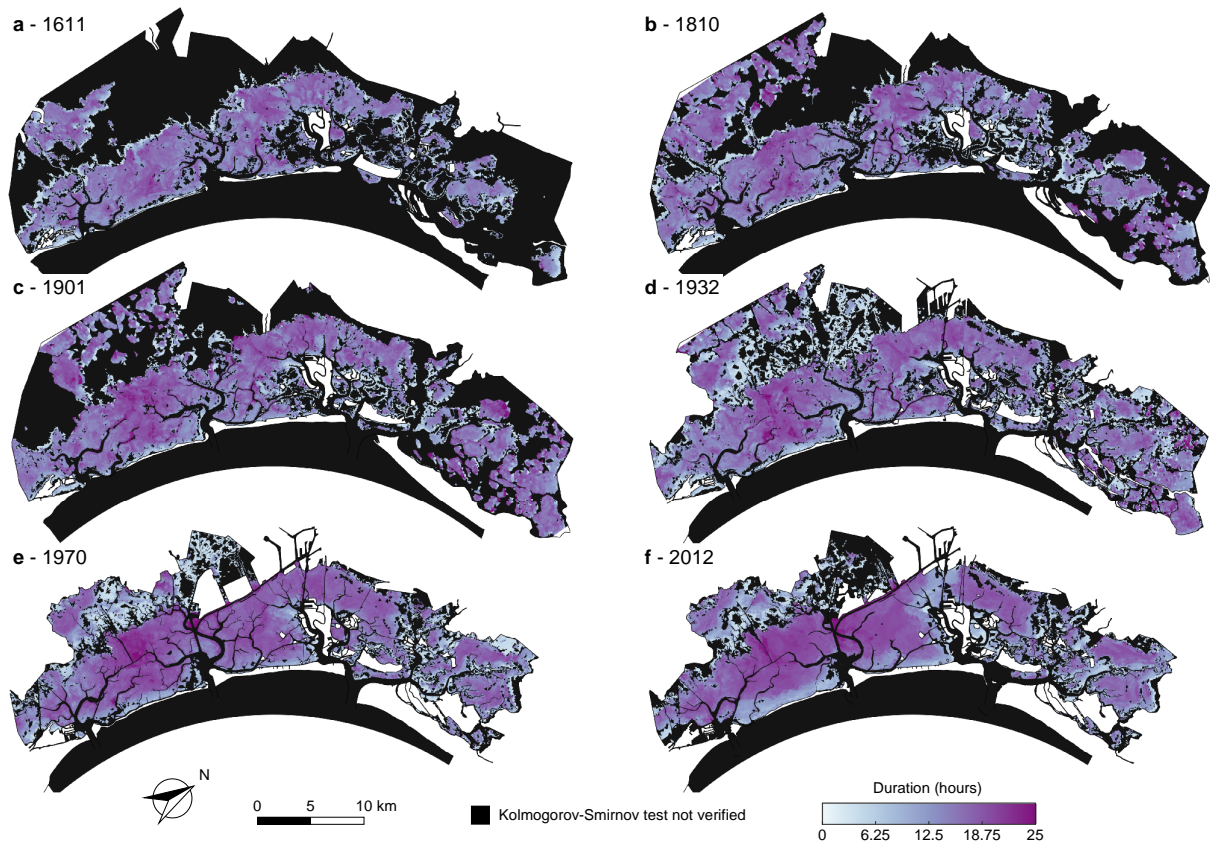


**Figure 5. Mean durations of over-threshold SSC events.** Spatial distribution of mean durations of over-threshold exceedances at sites where SSC events can be modeled as a marked Poisson process, as confirmed by the KS test ( $\alpha = 0.05$ ) for the six different configurations of the Venice Lagoon: 1611 (a), 1810 (b), 1901 (c), 1932 (d), 1970 (e), and 2012 (f).

the lagoon, where, because of the deepening experienced in the last century, the number of events able to resuspend sediments from the bottom decreased importantly, hence increasing the mean interarrival time of intense SSC events. In fact, over the central-southern shallow tidal flats of the four most ancient configurations, interarrival times present relatively low values (about 10 days), whereas they generally become longer (between 20 and 25 days) in the same areas in the more recent configurations. On the contrary, in the better preserved, northern portion of the lagoon, where the fetch is continuously interrupted by islands, spits, and salt marshes also in the more recent configurations, the mean interarrival times experienced only slight changes over centuries. As an example, Figure 6a shows the mean interarrival times,  $\lambda_t$ , experienced by the “Palude Maggiore” tidal flat (station S1 in Figure 1) that do not vary remarkably over time. On the contrary, the subtidal flat at the watershed divide between the Chioggia and Malamocco inlets, known as “Fondo dei Sette Morti” (station S2 in Figure 1), display a much larger variation of  $\lambda_t$  with decreasing interarrival times through centuries (Figure 6d). In the more ancient configurations, thanks to its relatively lower depth and its position sheltered by shallower tidal flats, the station S2 experienced over-threshold events



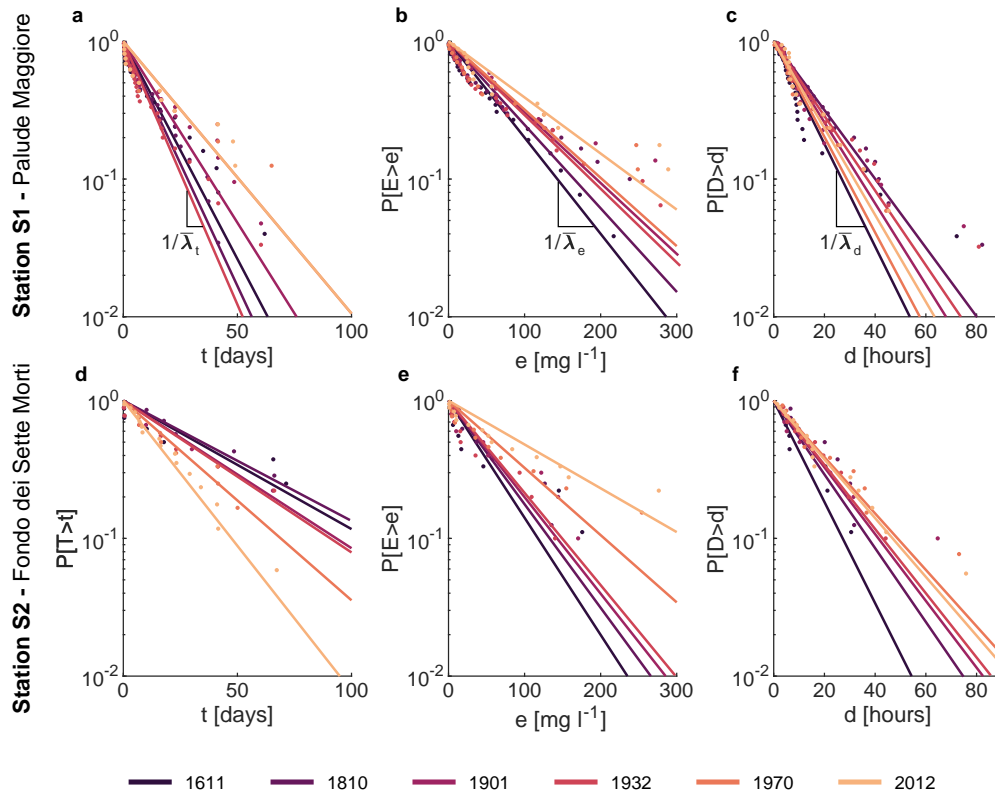


**Figure 6. Over-threshold SSC events at stations S1 and S2.** Statistical characterizations of over-threshold events at two stations S1 “Palude Maggiore” and S2 “Fondo dei Sette Morti” (see Figure 1a for locations) in the six configurations of the Venice Lagoon. Probability distributions of (a-b) interarrival times,  $t$ ; (c-d) intensities of peak excesses of over-threshold exceedances,  $e$ ; and (e-f) durations of over-threshold event,  $d$ .  $\bar{\lambda}_t$  mean interarrival time,  $\bar{\lambda}_e$  mean peak excess intensity, and  $\bar{\lambda}_d$  mean duration.

only during severe events. In the more recent configurations, over-threshold events become more frequent due to the deepening of the surrounding tidal flats, thus allowing larger waves and currents to propagate in this area and enhancing resuspension as well as suspended sediment transport.

The intensity of over-threshold events abruptly increases between 1932 and 1970 (Figure 4 and S5b). Indeed, SSC exceedance intensity maintains low mean values, generally below  $60 \text{ mg l}^{-1}$ , in all the configurations until 1932, thereafter it doubles on wide tidal-flat areas, especially in the central-southern lagoon and northwest of the city of Venice, where the action of wind waves is stronger because of the generalized deepening of those areas. This analysis confirms that the intensity increase is much more important in the central lagoon (station S2, Figure 6e) than in the northern part (station S1, Figure 6b).

Overall, over-threshold event durations slightly increase through the centuries (Figure 5 and S5c). However, two different trends can be distinguished in different portions of the lagoon, likewise interarrival times and intensities. The duration increase

285 in the more pristine, northern portion of the basin is much lower than that in the central and southern lagoon due to the heavier morphological modifications the latter areas experienced (Figure 6c and f).

SSC dynamics are affected by local entrainment and advection/dispersion processes from and toward the surrounding areas. Furthermore, the local resuspension is highly influenced by the combined effect of tidal currents and wind waves, thus depending on current velocity, water depth, fetch, wind intensity and duration (Fagherazzi and Wiberg, 2009; Carniello et al., 2016).  
290 As a consequence, the mean values of the random variables characterizing SSC events present highly heterogeneous spatial patterns in the more ancient configurations of the Venice Lagoon due to their higher morphological complexity.

To describe the relationship between interarrival times, durations and intensities, the temporal cross-correlation between these three random variables was computed for each point within the six configurations of the Venice Lagoon (Figure S6, S7, S8). Duration of over-threshold exceedances and intensity of peak excesses are highly correlated in all the six considered  
295 configurations, suggesting that longer events are linked to more intense ones (Figure S6 and S9a). On the contrary, durations and interarrival times, as well as intensities and interarrival times display almost no correlation (Figure S6, S7 and S9b,c). These relations between interarrival time, intensity and duration back up the idea that, as for BSS dynamics (D'Alpaos et al., Companion paper), over-threshold SSC events can be modeled as a 3-D Poisson process in which the marks (intensity and duration of over-threshold events) are mutually dependent but independent on interarrival times.

300 As a result of the cause-effect relationship between the BSS (cause) and SSC (effect), their spatial and temporal dynamics show a high cross-correlation between interarrival times (Figure 7), intensity (Figure 8) and duration (Figure 9) of BSS and SSC over-threshold events. Recalling the absence of correlation between interarrival times and both intensities and durations for both BSS and SSC events, we can conclude that, when generating synthetic time series, interarrival times of BSS and SSC events are mutually dependent but not related to their intensity and duration. Intensities and durations of SSC are instead  
305 strongly correlated with the corresponding properties of BSS events.

Despite showing high similarity and correlation, BSS and SSC events are not identical. The BSS ultimately depends on the local hydrodynamics, i.e. the local value of the bed shear stress  $\tau_{wc}$  produced by tidal currents and wind waves. On the contrary, the SSC is not only a function of the local entrainment but also of the suspended sediment flux from and towards the surrounding areas. As a result of the advection/dispersion processes, the spatial pattern of SSC is smoother than that of BSS.

310 The statistical characterization of over-threshold SSC events using their mean interarrival times, intensities and durations can be useful to estimate the total amount of reworked sediments. Although different portions of the lagoon experience different trends in these parameters depending on specific morphological modifications, a spatial average over the whole area where over-threshold SSC events can be described as Poisson processes shows that globally mean interarrival times and duration slightly vary and remain almost equal to about 30 days and 13 hours, respectively (Figure S5a and c). By contrast, intensity of  
315 the peak excess abruptly changes between 1932 and 1970. Between 1611 and 1932 the mean intensity maintains a value lower than  $45 \text{ mg l}^{-1}$ , but increases to  $64 \text{ mg l}^{-1}$  in 1970 and further to  $73 \text{ mg l}^{-1}$  in 2012 (Figure S5b).

This increase in the intensity of over-threshold SSC events, clearly associated with the generalized deepening of the tidal-flat areas, generates an increase in the amount of reworked sediments. This means that on average every month, for about 13 hours, the amount of sediment mobilized within the basin increases from about  $2 \cdot 10^6 \text{ kg}$  in the three most ancient configurations

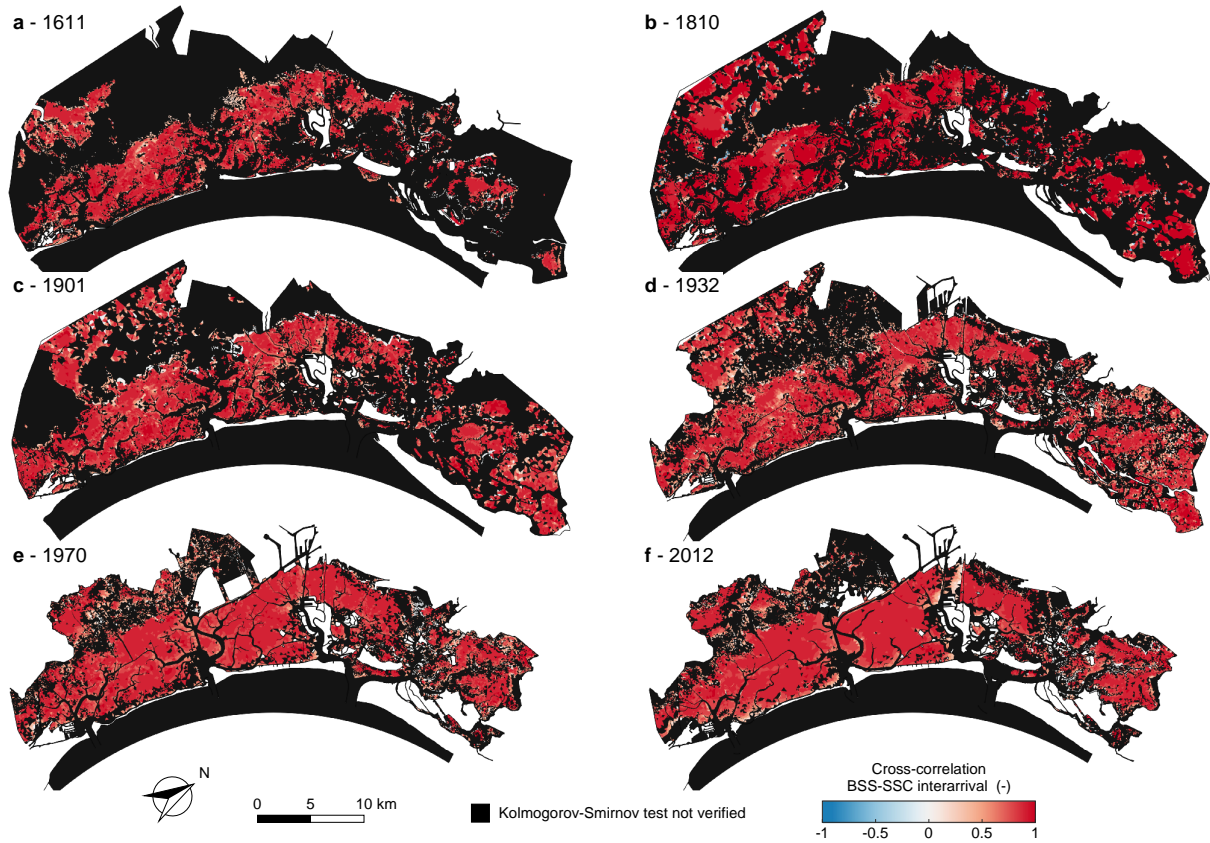


**Figure 7. Cross-correlation between interarrival times of over-threshold BSS and SSC events.** Spatial distribution of the cross-correlation between interarrival times of over-threshold BSS and SSC exceedances for the six different configurations of the Venice Lagoon: 1611 (a), 1810 (b), 1901 (c), 1932 (d), 1970 (e), and 2012 (f). Black identifies sites where over-threshold BSS or SSC events cannot be modeled as a marked Poisson process (i.e. the KS test is not verified for the interarrival time).

320 to more than  $6.8 \cdot 10^6$  kg in the 2012 configuration (Table 1). Besides directly boosting the amount of sediment available for export toward the open sea given the ebb-dominated character of the Venice Lagoon (Ferrarin et al., 2015; Finotello et al., 2022), the increase of suspended sediment also affects numerous biological and ecological processes that in turn influence the morphological evolution of the tidal system (e.g., Venier et al., 2014; Pivato et al., 2019).

325 As already mentioned, modeling the morphodynamic evolution of tidal landscapes over long timescales (decades or centuries) necessarily requires the use of simplified approaches. However, a classical assumption of long-term evolution models is that the sediment supply is constant or monotonically related to mean water depth. The results presented in this study, together with those obtained for erosion events (D’Alpaos et al., Companion paper), demonstrate that the time series of both BSS and SSC can be described as marked Poisson processes with exponentially distributed interarrival times, intensities, and durations, thereby setting a framework for the synthetic generation of statistically significant external forcing factors (shear

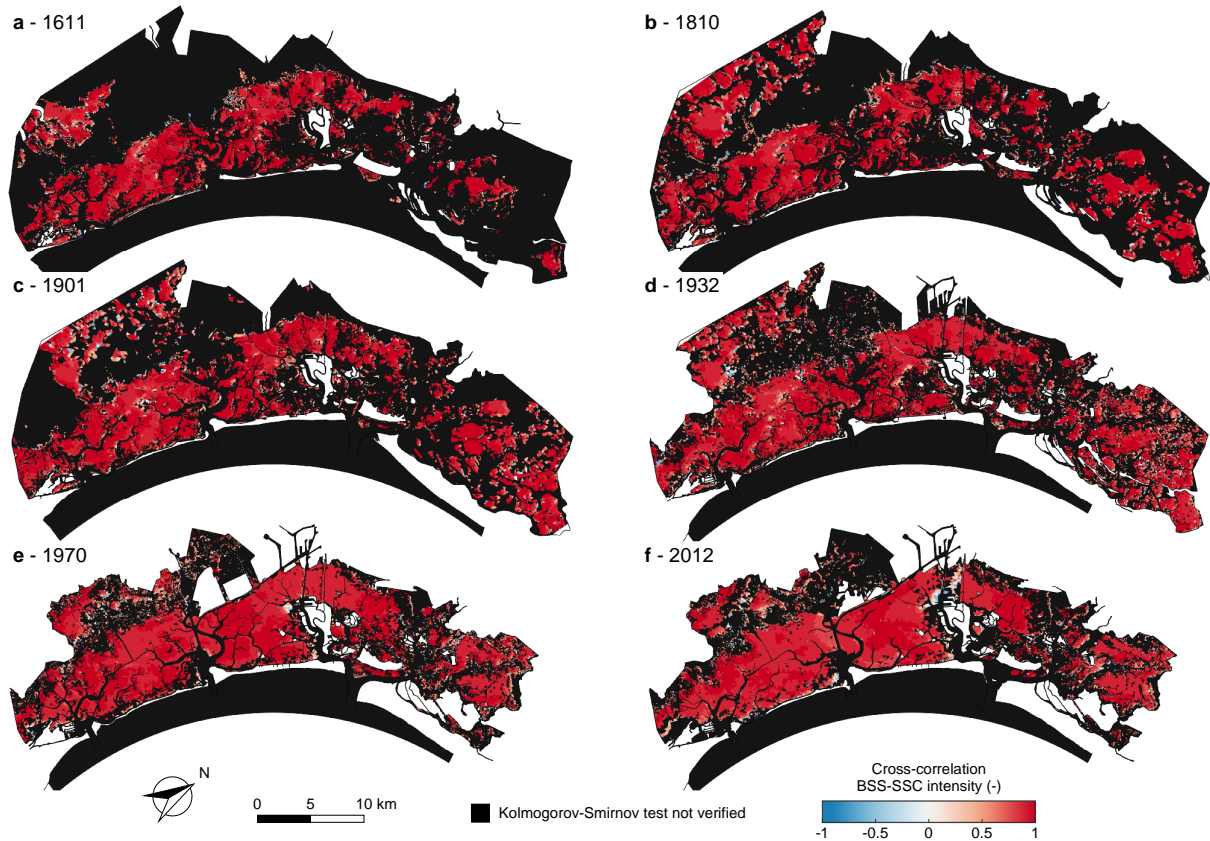


**Figure 8. Cross-correlation between intensities of over-threshold BSS and SSC events.** Spatial distribution of the cross-correlation between intensities of over-threshold exceedances BSS and SSC for the six different configurations of the Venice Lagoon: 1611 (a), 1810 (b), 1901 (c), 1932 (d), 1970 (e), and 2012 (f). Black identifies sites where over-threshold BSS or SSC events cannot be modeled as a marked Poisson process (i.e. the KS test is not verified for the interarrival time).

330 stress at the bottom and suspended sediment available in the water column) that should improve the reliability of long-term biomorphodynamic models with a limited increase in the number of parameters.

#### 4 Conclusions

SSC dynamics in shallow tidal environments is usually investigated by means of field measurements or remote sensing analysis. However, due to the limited spatial coverage of field measurement and the temporal resolution of satellite images, long-term  
 335 SSC dynamics at the basin scale are seldom available. Numerical models, once properly calibrated and tested, can provide reliable long SSC time series which can be used to statistically characterize the spatial and temporal variability of intense SSC events.

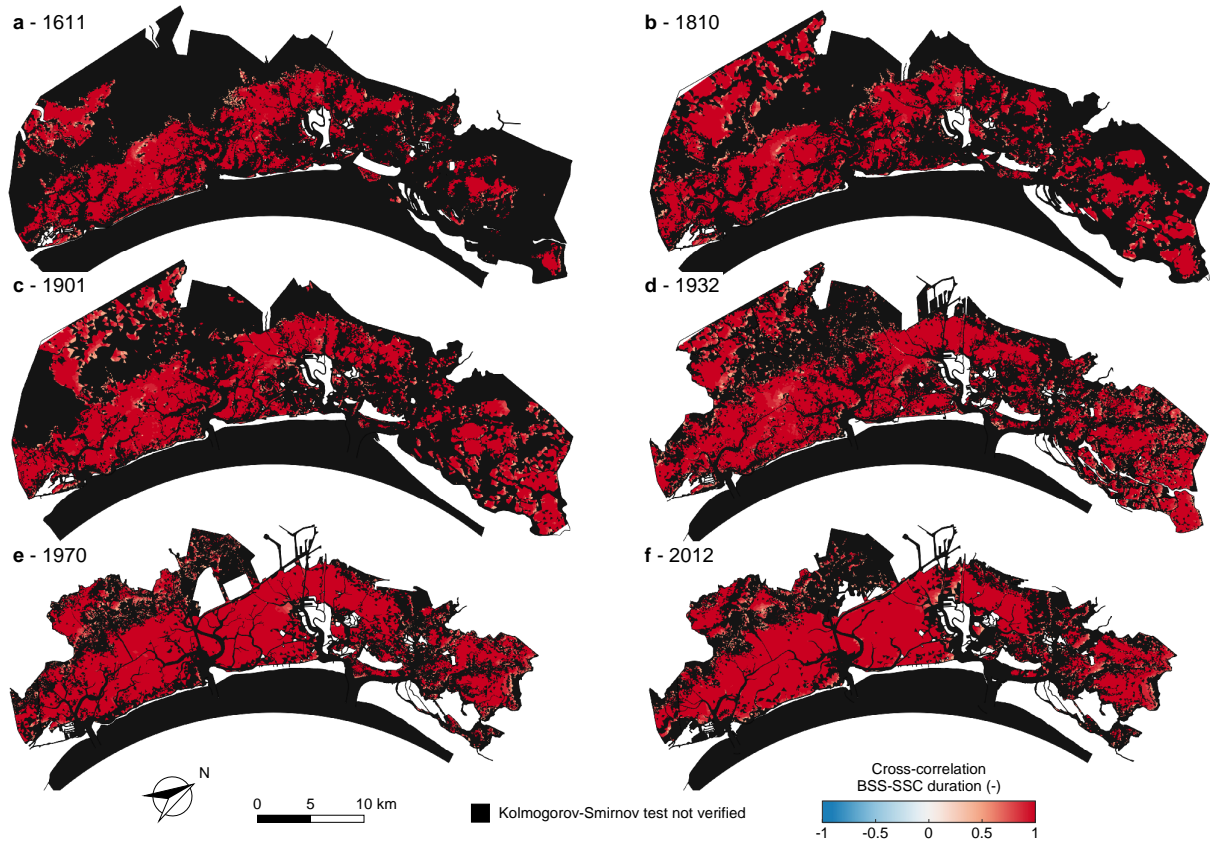


**Figure 9. Cross-correlation between durations of over-threshold BSS and SSC events.** Spatial distribution of the cross-correlation between durations of over-threshold exceedances BSS and SSC for the six different configurations of the Venice Lagoon: 1611 (a), 1810 (b), 1901 (c), 1932 (d), 1970 (e), and 2012 (f). Black identifies sites where over-threshold BSS or SSC events cannot be modeled as a marked Poisson process (i.e. the KS test is not verified for the interarrival time).

In the present study, we applied a custom-built, extensively tested, 2-D finite-element numerical model to reproduce SSC dynamics at basin scale in six historical configurations of the Venice Lagoon, covering a time span of four centuries. The computed SSC time series were analysed on the basis of the peak-over-threshold theory. Statistical analyses suggest that over-threshold SSC events can be modelled as a marked Poisson process over wide areas of all the selected configurations of the Venice Lagoon.

We found that, due to the morphological evolution experienced by the lagoon in the last four centuries, mean interarrival time, intensity and duration of over-threshold events generally increase through the centuries as a consequence of the morphological evolution of the shallow tidal environment, generating slightly less frequent and longer, but stronger, resuspension events.

Furthermore, almost no correlation is shown to exist between durations and interarrival times of over-threshold exceedances and between intensities and interarrival times, whereas the intensity of peak excesses and duration are highly correlated. This

**Table 1. Sediment reworking in the historical configurations of the Venice Lagoon.** *area* (km<sup>2</sup>): area of the lagoon where KS is verified; *h* (m): mean water depth of the area; *V<sub>w</sub>* (10<sup>6</sup> m<sup>3</sup>): mean volume of water, obtained as product of area and water depth; *e* (mg l<sup>-1</sup>): mean intensity of over-threshold SSC events; *S<sub>mob</sub>* (10<sup>6</sup> kg): sediment mobilized, assuming a triangular-shaped temporal evolution of over-threshold SSC events, with peak excess *e*.

Year	area (km <sup>2</sup> )	h (m)	V <sub>w</sub> (10 <sup>6</sup> m <sup>3</sup> )	<i>e</i> (mg l <sup>-1</sup> )	S <sub>mob</sub> (10 <sup>6</sup> kg)
1611	226.882	0.59	134.403	44.20	1.980
1810	294.649	0.43	127.022	40.84	1.729
1901	307.951	0.47	143.985	42.66	2.047
1932	350.166	0.54	188.661	43.49	2.734
1970	283.196	0.77	217.863	64.16	4.659
2012	270.022	1.04	279.969	73.21	6.832

confirms that resuspension events can be modeled as a 3-D marked Poisson process with marks (intensity and duration) mutually dependent but independent on the interarrival times in all the historical configurations of the Venice Lagoon. Moreover, a comparison with the analysis of over-threshold BSS events shows that interarrival times, intensities and durations of both BSS and SSC events are mutually related.

These findings, together with those obtained for BSS events (D’Alpaos et al., Companion paper), provide the basis to develop a theoretical framework for generating synthetic, yet statistically realistic, forcings to be used in the long-term morphodynamic modeling of shallow tidal environments, in general, and for the Venice Lagoon, in particular.

*Data availability.* All data presented in this study and used for the analysis of the suspended sediment concentration are available at <https://researchdata.cab.unipd.it/id/eprint/729> (10.25430/researchdata.cab.unipd.it.00000729)

*Author contributions.* Conceptualization: Davide Tognin, Andrea D’Alpaos, Andrea Rinaldo, Luca Carniello;  
Methodology: Davide Tognin, Andrea D’Alpaos, Luca Carniello;  
Formal analysis and investigation: Davide Tognin;  
Figures: Davide Tognin;  
Writing - original draft preparation: Davide Tognin;  
Writing - review and editing: all authors;  
Funding acquisition: Andrea D’Alpaos, Luca Carniello;  
Resources: Andrea D’Alpaos, Luca Carniello, Luigi D’Alpaos, Andrea Rinaldo;  
Supervision: Andrea D’Alpaos, Luca Carniello.

*Competing interests.* The authors declare no competing interests.

*Acknowledgements.* This scientific activity was partially performed as part of the Research Programme Venezia2021, with contributions from the Provveditorato for the Public Works of Veneto, Trentino Alto Adige and Friuli Venezia Giulia, provided through the concessionary of State Consorzio Venezia Nuova and coordinated by CORILA, Research Line 3.2 (PI A.D.), by the 2019 University of Padova project (BIRD199419) ‘Tidal network ontogeny and evolution: a comprehensive approach based on laboratory experiments with ancillary numerical modelling and field measurements’ (PI L.C.), and by University of Padova SID2021 project, ‘Unraveling Carbon Sequestration Potential by Salt-Marsh Ecosystems’ (P.I. A. D.).



## References

- Anderson, F. E.: Resuspension of estuarine sediments by small amplitude waves, *Journal of Sedimentary Research*, 42, 602–607, 1972.
- 375 Balkema, A. A. and de Haan, L.: Residual Life Time at Great Age, *The Annals of Probability*, <https://doi.org/10.1214/aop/1176996548>, 1974.
- Bertassello, L. E., Rao, P. S. C., Park, J., Jawitz, J. W., and Botter, G.: Stochastic modeling of wetland-groundwater systems, *Advances in Water Resources*, 112, 214–223, <https://doi.org/10.1016/j.advwatres.2017.12.007>, 2018.
- Botter, G., Basso, S., Rodriguez-Iturbe, I., and Rinaldo, A.: Resilience of river flow regimes, *Proceedings of the National Academy of Sciences*, 110, 12 925–12 930, <https://doi.org/10.1073/pnas.1311920110>, 2013.
- 380 Brand, E., Chen, M., and Montreuil, A.-L.: Optimizing measurements of sediment transport in the intertidal zone, *Earth-Science Reviews*, 200, 103 029, <https://doi.org/10.1016/j.earscirev.2019.103029>, 2020.
- Breugem, W. A. and Holthuijsen, L. H.: Generalized Shallow Water Wave Growth from Lake George, *Journal of Waterway, Port, Coastal, and Ocean Engineering*, [https://doi.org/10.1061/\(asce\)0733-950x\(2007\)133:3\(173\)](https://doi.org/10.1061/(asce)0733-950x(2007)133:3(173)), 2007.
- 385 Carniello, L., Defina, A., Fagherazzi, S., and D’Alpaos, L.: A combined wind wave-tidal model for the Venice lagoon, Italy, *Journal of Geophysical Research: Earth Surface*, 110, 1–15, <https://doi.org/10.1029/2004JF000232>, 2005.
- Carniello, L., Defina, A., and D’Alpaos, L.: Morphological evolution of the Venice lagoon: Evidence from the past and trend for the future, *Journal of Geophysical Research*, 114, F04 002, <https://doi.org/10.1029/2008JF001157>, 2009.
- Carniello, L., D’Alpaos, A., and Defina, A.: Modeling wind waves and tidal flows in shallow micro-tidal basins, *Estuarine, Coastal and Shelf Science*, 92, 263–276, <https://doi.org/10.1016/j.ecss.2011.01.001>, 2011.
- 390 Carniello, L., Defina, A., and D’Alpaos, L.: Modeling sand-mud transport induced by tidal currents and wind waves in shallow microtidal basins: Application to the Venice Lagoon (Italy), *Estuarine, Coastal and Shelf Science*, 102–103, 105–115, <https://doi.org/10.1016/j.ecss.2012.03.016>, 2012.
- Carniello, L., Silvestri, S., Marani, M., D’Alpaos, A., Volpe, V., and Defina, A.: Sediment dynamics in shallow tidal basins: In situ observations, satellite retrievals, and numerical modeling in the Venice Lagoon, *Journal of Geophysical Research: Earth Surface*, 119, 802–815, <https://doi.org/10.1002/2013JF003015>, 2014.
- 395 Carniello, L., D’Alpaos, A., Botter, G., and Rinaldo, A.: Statistical characterization of spatiotemporal sediment dynamics in the Venice lagoon, *Journal of Geophysical Research: Earth Surface*, pp. 1049–1064, <https://doi.org/10.1002/2015JF003793>, 2016.
- Carr, J. A., D’Odorico, P., McGlathery, K. J., and Wiberg, P. L.: Stability and bistability of seagrass ecosystems in shallow coastal lagoons: Role of feedbacks with sediment resuspension and light attenuation, *Journal of Geophysical Research: Biogeosciences*, 115, <https://doi.org/10.1029/2009JG001103>, 2010.
- 400 Carr, J. A., D’Odorico, P., McGlathery, K. J., and Wiberg, P. L.: Spatially explicit feedbacks between seagrass meadow structure, sediment and light: Habitat suitability for seagrass growth, *Advances in Water Resources*, 93, 315–325, <https://doi.org/https://doi.org/10.1016/j.advwatres.2015.09.001>, 2016.
- 405 Chen, X., Zhang, C., Paterson, D. M., Townend, I., Jin, C., Zhou, Z., Gong, Z., and Feng, Q.: The effect of cyclic variation of shear stress on non-cohesive sediment stabilization by microbial biofilms: the role of ‘biofilm precursors’, *Earth Surface Processes and Landforms*, 44, 1471–1481, <https://doi.org/10.1002/esp.4573>, 2019.
- Christiansen, T., Wiberg, P. L., and Milligan, T. G.: Flow and Sediment Transport on a Tidal Salt Marsh Surface, *Estuarine, Coastal and Shelf Science*, 50, 315–331, <https://doi.org/10.1006/ecss.2000.0548>, 2000.



- 410 Cramér, H. and Leadbetter, M. R.: Stationary and related stochastic processes, John Wiley & Sons, Ltd, New York, 1967.
- D'Alpaos, A. and Marani, M.: Reading the signatures of biologic-geomorphic feedbacks in salt-marsh landscapes, *Advances in Water Resources*, 93, 265–275, <https://doi.org/10.1016/j.advwatres.2015.09.004>, 2016.
- D'Alpaos, A., Lanzoni, S., Marani, M., and Rinaldo, A.: Landscape evolution in tidal embayments: Modeling the interplay of erosion, sedimentation, and vegetation dynamics, *Journal of Geophysical Research*, 112, F01 008, <https://doi.org/10.1029/2006JF000537>, 2007.
- 415 D'Alpaos, A., Mudd, S. M., and Carniello, L.: Dynamic response of marshes to perturbations in suspended sediment concentrations and rates of relative sea level rise, *Journal of Geophysical Research: Earth Surface*, 116, 1–13, <https://doi.org/10.1029/2011JF002093>, 2011.
- D'Alpaos, A., Carniello, L., and Rinaldo, A.: Statistical mechanics of wind wave-induced erosion in shallow tidal basins: Inferences from the Venice Lagoon, *Geophysical Research Letters*, <https://doi.org/10.1002/grl.50666>, 2013.
- D'Alpaos, A., Tognin, D., Tommasini, L., D'Alpaos, L., Rinaldo, A., and Carniello, L.: Statistical characterization of erosion and sediment  
420 transport mechanics in shallow tidal environments. Part 1: erosion dynamics, Companion paper.
- D'Alpaos, L.: Fatti e misfatti di idraulica lagunare. La laguna di Venezia dalla diversione dei fiumi alle nuove opere delle bocche di porto, Istituto Veneto di Scienze, Lettere e Arti, Venice, 2010.
- Defina, A.: Two-dimensional shallow flow equations for partially dry areas, *Water Resources Research*, 36, 3251–3264, <https://doi.org/10.1029/2000WR900167>, 2000.
- 425 D'Odorico, P. and Fagherazzi, S.: A probabilistic model of rainfall-triggered shallow landslides in hollows: A long-term analysis, *Water Resources Research*, <https://doi.org/10.1029/2002WR001595>, 2003.
- Dyer, K. R.: Sediment processes in estuaries: Future research requirements, *Journal of Geophysical Research*, 94, 14 327, <https://doi.org/10.1029/JC094iC10p14327>, 1989.
- Dyer, K. R., Christie, M. C., Feates, N., Fennessy, M. J., Pejrup, M., and van der Lee, W.: An Investigation into Processes Influencing the  
430 Morphodynamics of an Intertidal Mudflat, the Dollard Estuary, The Netherlands: I. Hydrodynamics and Suspended Sediment, *Estuarine, Coastal and Shelf Science*, 50, 607–625, <https://doi.org/10.1006/ecss.1999.0596>, 2000.
- Fagherazzi, S. and Wiberg, P. L.: Importance of wind conditions, fetch, and water levels on wave-generated shear stresses in shallow intertidal basins, *Journal of Geophysical Research: Earth Surface*, <https://doi.org/10.1029/2008JF001139>, 2009.
- Ferrarin, C., Tomasin, A., Bajo, M., Petrizzo, A., and Umgiesser, G.: Tidal changes in a heavily modified coastal wetland, *Continental Shelf  
435 Research*, 101, 22–33, <https://doi.org/10.1016/j.csr.2015.04.002>, 2015.
- Finotello, A., Tognin, D., Carniello, L., Ghinassi, M., Bertuzzo, E., and D'Alpaos, A.: Hydrodynamic feedbacks of salt-marsh loss in shallow microtidal back-barrier systems, *Earth and Space Science Open Archive*, p. 32, <https://doi.org/10.1002/essoar.10511787.2>, 2022.
- Friedrichs, C. T. and Madsen, O. S.: Nonlinear diffusion of the tidal signal in frictionally dominated embayments, *Journal of Geophysical Research*, 97, 5637, <https://doi.org/10.1029/92jc00354>, 1992.
- 440 Gartner, J. W.: Estimating suspended solids concentrations from backscatter intensity measured by acoustic Doppler current profiler in San Francisco Bay, California, *Marine Geology*, 211, 169–187, <https://doi.org/10.1016/j.margeo.2004.07.001>, 2004.
- Goodwin, G. C. H., Marani, M., Silvestri, S., Carniello, L., and D'Alpaos, A.: Toward coherent space-time mapping of seagrass cover from satellite data: example of a Mediterranean lagoon, *EGUsphere*, 2023, 1–32, <https://doi.org/10.5194/egusphere-2022-1501>, 2023.
- Grass, A. J.: Initial Instability of Fine Bed Sand, *Journal of the Hydraulics Division*, 96, 619–632, <https://doi.org/10.1061/JYCEAJ.0002369>,  
445 1970.
- Green, M. O.: Very small waves and associated sediment resuspension on an estuarine intertidal flat, *Estuarine, Coastal and Shelf Science*, 93, 449–459, <https://doi.org/10.1016/j.ecss.2011.05.021>, 2011.

- Green, M. O. and Coco, G.: Sediment transport on an estuarine intertidal flat: Measurements and conceptual model of waves, rainfall and exchanges with a tidal creek, *Estuarine, Coastal and Shelf Science*, <https://doi.org/10.1016/j.ecss.2006.11.006>, 2007.
- 450 Green, M. O. and Coco, G.: Review of wave-driven sediment resuspension and transport in estuaries, *Reviews of Geophysics*, 52, 77–117, <https://doi.org/10.1002/2013RG000437>, 2014.
- Green, M. O., Black, K. P., and Amos, C. L.: Control of estuarine sediment dynamics by interactions between currents and waves at several scales, *Marine Geology*, 144, 97–116, [https://doi.org/10.1016/S0025-3227\(97\)00065-0](https://doi.org/10.1016/S0025-3227(97)00065-0), 1997.
- Holthuijsen, L. H., Booij, N., and Herbers, T. H. C.: A prediction model for stationary, short-crested waves in shallow water with ambient  
455 currents, *Coastal Engineering*, 13, 23–54, [https://doi.org/https://doi.org/10.1016/0378-3839\(89\)90031-8](https://doi.org/https://doi.org/10.1016/0378-3839(89)90031-8), 1989.
- Hughes, Z. J.: Tidal Channels on Tidal Flats and Marshes, in: *Principles of Tidal Sedimentology*, edited by Davis, R. and Dalrymple, R., chap. 11, pp. 1–621, Springer, <https://doi.org/10.1007/978-94-007-0123-6>, 2012.
- Kirwan, M. L. and Murray, A. B.: A coupled geomorphic and ecological model of tidal marsh evolution, *Proceedings of the National Academy of Sciences of the United States of America*, 104, 6118–6122, <https://doi.org/10.1073/pnas.0700958104>, 2007.
- 460 Lawson, S. E., Wiberg, P. L., McGlathery, K. J., and Fugate, D. C.: Wind-driven sediment suspension controls light availability in a shallow coastal lagoon, *Estuaries and Coasts*, 30, 102–112, <https://doi.org/10.1007/BF02782971>, 2007.
- Le Hir, P., Monbet, Y., and Orvain, F.: Sediment erodability in sediment transport modelling: Can we account for biota effects?, *Continental Shelf Research*, 27, 1116–1142, <https://doi.org/10.1016/j.csr.2005.11.016>, 2007.
- Maciel, F. P., Santoro, P. E., and Pedocchi, F.: Spatio-temporal dynamics of the Río de la Plata turbidity front; combining remote sensing with in-situ measurements and numerical modeling, *Continental Shelf Research*, 213, 104301, <https://doi.org/https://doi.org/10.1016/j.csr.2020.104301>, 2021.
- Marani, M., Da Lio, C., and D’Alpaos, A.: Vegetation engineers marsh morphology through multiple competing stable states, *Proceedings of the National Academy of Sciences*, <https://doi.org/10.1073/pnas.1218327110>, 2013.
- Martini, P., Carniello, L., and Avanzi, C.: Two dimensional modelling of flood flows and suspended sediment transport: the case of the Brenta  
470 River, Veneto (Italy), *Natural Hazards and Earth System Sciences*, 4, 165–181, <https://doi.org/10.5194/nhess-4-165-2004>, 2004.
- Masselink, G., Hughes, M., and Knight, J.: *Introduction to Coastal Processes and Geomorphology*, Routledge, <https://doi.org/10.4324/9780203785461>, 2014.
- McSweeney, J. M., Chant, R. J., Wilkin, J. L., and Sommerfield, C. K.: Suspended-Sediment Impacts on Light-Limited Productivity in the Delaware Estuary, *Estuaries and Coasts*, 40, 977–993, <https://doi.org/10.1007/s12237-016-0200-3>, 2017.
- 475 Miller, R. L. and McKee, B. A.: Using MODIS Terra 250 m imagery to map concentrations of total suspended matter in coastal waters, *Remote Sensing of Environment*, 93, 259–266, <https://doi.org/https://doi.org/10.1016/j.rse.2004.07.012>, 2004.
- Möller, I., Spencer, T., French, J. R., Leggett, D. J., and Dixon, M.: Wave transformation over salt marshes: A field and numerical modelling study from north Norfolk, England, *Estuarine, Coastal and Shelf Science*, <https://doi.org/10.1006/ecss.1999.0509>, 1999.
- Moore, K. A. and Wetzel, R. L.: Seasonal variations in eelgrass (*Zostera marina* L.) responses to nutrient enrichment and  
480 reduced light availability in experimental ecosystems, *Journal of Experimental Marine Biology and Ecology*, 244, 1–28, [https://doi.org/https://doi.org/10.1016/S0022-0981\(99\)00135-5](https://doi.org/https://doi.org/10.1016/S0022-0981(99)00135-5), 2000.
- Murray, A. B.: Reducing model complexity for explanation and prediction, *Geomorphology*, 90, 178–191, <https://doi.org/10.1016/j.geomorph.2006.10.020>, 2007.
- Nepf, H. M.: Drag, turbulence, and diffusion in flow through emergent vegetation, *Water Resources Research*, 35, 479–489,  
485 <https://doi.org/10.1029/1998WR900069>, 1999.

- Nichols, M. M. and Boon, J. D.: Sediment Transport Processes in Coastal Lagoons, in: Coastal Lagoon Processes, edited by Kjerfve, B., C, chap. 7, pp. 157–219, Elsevier, [https://doi.org/10.1016/S0422-9894\(08\)70012-6](https://doi.org/10.1016/S0422-9894(08)70012-6), 1994.
- Ouillon, S., Douillet, P., and Andréfouët, S.: Coupling satellite data with in situ measurements and numerical modeling to study fine suspended sediment transport: a study for the lagoon of New Caledonia, *Coral Reefs*, 23, 109–122, <https://doi.org/10.1007/s00338-003-0352-z>, 2004.
- Park, J., Botter, G., Jawitz, J. W., and Rao, P. S. C.: Stochastic modeling of hydrologic variability of geographically isolated wetlands: Effects of hydro-climatic forcing and wetland bathymetry, *Advances in Water Resources*, <https://doi.org/10.1016/j.advwatres.2014.03.007>, 2014.
- Parsons, D. R., Schindler, R. J., Hope, J. A., Malarkey, J., Baas, J. H., Peakall, J., Manning, A. J., Ye, L., Simmons, S., Paterson, D. M., Aspden, R. J., Bass, S. J., Davies, A. G., Lichtman, I. D., and Thorne, P. D.: The role of biophysical cohesion on subaqueous bed form size, *Geophysical Research Letters*, 43, 1566–1573, <https://doi.org/10.1002/2016GL067667>, 2016.
- Pivato, M., Carniello, L., Moro, I., and D’Odorico, P.: On the feedback between water turbidity and microphytobenthos growth in shallow tidal environments, *Earth Surface Processes and Landforms*, 44, 1192–1206, <https://doi.org/10.1002/esp.4567>, 2019.
- Ralston, D. K. and Stacey, M. T.: Tidal and meteorological forcing of sediment transport in tributary mudflat channels, *Continental Shelf Research*, 27, 1510–1527, <https://doi.org/10.1016/j.csr.2007.01.010>, 2007.
- Rodriguez-Iturbe, I., Cox, D. R., and Isham, V.: Some models for rainfall based on stochastic point processes, *Proceedings of the Royal Society of London. A. Mathematical and Physical Sciences*, 410, 269–288, <https://doi.org/10.1098/rspa.1987.0039>, 1987.
- Roner, M., D’Alpaos, A., Ghinassi, M., Marani, M., Silvestri, S., Franceschinis, E., and Realdon, N.: Spatial variation of salt-marsh organic and inorganic deposition and organic carbon accumulation: Inferences from the Venice lagoon, Italy, *Advances in Water Resources*, <https://doi.org/10.1016/j.advwatres.2015.11.011>, 2016.
- Ruhl, C. A., Schoellhamer, D. H., Stumpf, R. P., and Lindsay, C. L.: Combined Use of Remote Sensing and Continuous Monitoring to Analyse the Variability of Suspended-Sediment Concentrations in San Francisco Bay, California, *Estuarine, Coastal and Shelf Science*, 53, 801–812, <https://doi.org/10.1006/ecss.2000.0730>, 2001.
- Sanford, L. P.: Wave-Forced Resuspension of Upper Chesapeake Bay Muds, *Estuaries*, 17, 148, <https://doi.org/10.2307/1352564>, 1994.
- Sarretta, A., Pillon, S., Molinaroli, E., Guerzoni, S., and Fontolan, G.: Sediment budget in the Lagoon of Venice, Italy, *Continental Shelf Research*, 30, 934–949, <https://doi.org/10.1016/j.csr.2009.07.002>, 2010.
- Soulsby, R. L.: Bed shear-stresses due to combined waves and currents, in: *Advances in Coastal Morphodynamics*, edited by Stive, M. J. F., pp. 420–423, Delft Hydraul., Delft, Netherlands, 1995.
- Soulsby, R. L.: *Dynamics of Marine Sands: A Manual for Practical Applications*, Thomas Telford, London, 1997.
- Tambroni, N., Figueiredo da Silva, J., Duck, R. W., McLelland, S. J., Venier, C., and Lanzoni, S.: Experimental investigation of the impact of macroalgal mats on the wave and current dynamics, *Advances in Water Resources*, 93, 326–335, <https://doi.org/10.1016/j.advwatres.2015.09.010>, 2016.
- Temmerman, S., Bouma, T. J., Govers, G., and Lauwaet, D.: Flow paths of water and sediment in a tidal marsh: Relations with marsh developmental stage and tidal inundation height, *Estuaries*, 28, 338–352, <https://doi.org/10.1007/BF02693917>, 2005.
- Temmerman, S., Bouma, T. J., Van De Koppel, J., van der Wal, D., de Vries, M. B., and Herman, P. M. J.: Vegetation causes channel erosion in a tidal landscape, *Geology*, 35, 631–634, <https://doi.org/10.1130/G23502A.1>, 2007.
- Tinoco, R. O. and Coco, G.: A laboratory study on sediment resuspension within arrays of rigid cylinders, *Advances in Water Resources*, 92, 1–9, <https://doi.org/10.1016/j.advwatres.2016.04.003>, 2016.

- Tognin, D., D'Alpaos, A., Marani, M., and Carniello, L.: Marsh resilience to sea-level rise reduced by storm-surge barriers in the Venice Lagoon, *Nature Geoscience*, 14, 906–911, <https://doi.org/10.1038/s41561-021-00853-7>, 2021.
- 525 Tognin, D., Finotello, A., D'Alpaos, A., Viero, D. P., Pivato, M., Mel, R. A., Defina, A., Bertuzzo, E., Marani, M., and Carniello, L.: Loss of geomorphic diversity in shallow tidal embayments promoted by storm-surge barriers, *Science Advances*, 8, eabm8446, <https://doi.org/10.1126/sciadv.abm8446>, 2022.
- Tommasini, L., Carniello, L., Ghinassi, M., Roner, M., and D'Alpaos, A.: Changes in the wind-wave field and related salt-marsh lateral erosion: inferences from the evolution of the Venice Lagoon in the last four centuries, *Earth Surface Processes and Landforms*, 44, 1633–  
530 1646, <https://doi.org/doi:10.1002/esp.4599>, 2019.
- van Ledden, M., Wang, Z. B., Winterwerp, H., and De Vriend, H. J.: Sand-mud morphodynamics in a short tidal basin, in: *Ocean Dynamics*, <https://doi.org/10.1007/s10236-003-0050-y>, 2004.
- Venier, C., D'Alpaos, A., and Marani, M.: Evaluation of sediment properties using wind and turbidity observations in the shallow tidal areas of the Venice Lagoon, *Journal of Geophysical Research: Earth Surface*, <https://doi.org/10.1002/2013JF003019>, 2014.
- 535 Volpe, V., Silvestri, S., and Marani, M.: Remote sensing retrieval of suspended sediment concentration in shallow waters, *Remote Sensing of Environment*, 115, 44–54, <https://doi.org/10.1016/j.rse.2010.07.013>, 2011.
- Vu, H. D., Wieszki, K., and Pennings, S. C.: Ecosystem engineers drive creek formation in salt marshes, *Ecology*, 98, 162–174, <https://doi.org/10.1002/ecy.1628>, 2017.
- Wang, P.: Principles of Sediment Transport Applicable in Tidal Environments, in: *Principles of Tidal Sedimentology*, edited by Davis, R. A. and Dalrymple, R. W., vol. c, pp. 1–621, Springer Netherlands, Dordrecht, <https://doi.org/10.1007/978-94-007-0123-6>, 2012.
- 540 Widdows, J. and Brinsley, M.: Impact of biotic and abiotic processes on sediment dynamics and the consequences to the structure and functioning of the intertidal zone, *Journal of Sea Research*, 48, 143–156, [https://doi.org/10.1016/S1385-1101\(02\)00148-X](https://doi.org/10.1016/S1385-1101(02)00148-X), 2002.
- Woodroffe, C. D.: *Coasts*, Cambridge University Press, Cambridge, <https://doi.org/10.1017/CBO9781316036518>, 2002.
- Wren, D. G., Barkdoll, B. D., Kuhnle, R. A., and Derrow, R. W.: Field Techniques for Suspended-Sediment Measurement, *Journal of*  
545 *Hydraulic Engineering*, 126, 97–104, [https://doi.org/10.1061/\(ASCE\)0733-9429\(2000\)126:2\(97\)](https://doi.org/10.1061/(ASCE)0733-9429(2000)126:2(97)), 2000.
- Young, I. R. and Verhagen, L. A.: The growth of fetch limited waves in water of finite depth. Part 1. Total energy and peak frequency, *Coastal Engineering*, [https://doi.org/10.1016/S0378-3839\(96\)00006-3](https://doi.org/10.1016/S0378-3839(96)00006-3), 1996.

# **Supplement for**

## **Statistical characterization of erosion and sediment transport mechanics in shallow tidal environments. Part 2: suspended sediment dynamics**

Davide Tognin<sup>1,2,\*</sup>, Andrea D'Alpaos<sup>2,\*</sup>, Luigi D'Alpaos<sup>1</sup>, Andrea Rinaldo<sup>1,3</sup>, and Luca Carniello<sup>1</sup>

<sup>1</sup>Department of Civil, Environmental, and Architectural Engineering, University of Padova, Padova, Italy

<sup>2</sup>Department of Geosciences, University of Padova, Padova, Italy

<sup>3</sup>Laboratory of Ecohydrology ECHO/IEE/ENAC, École Polytechnique Fédérale de Lausanne, Lausanne, Switzerland

\*These authors contributed equally to this work.

**Correspondence:** Davide Tognin (davide.tognin@unipd.it)

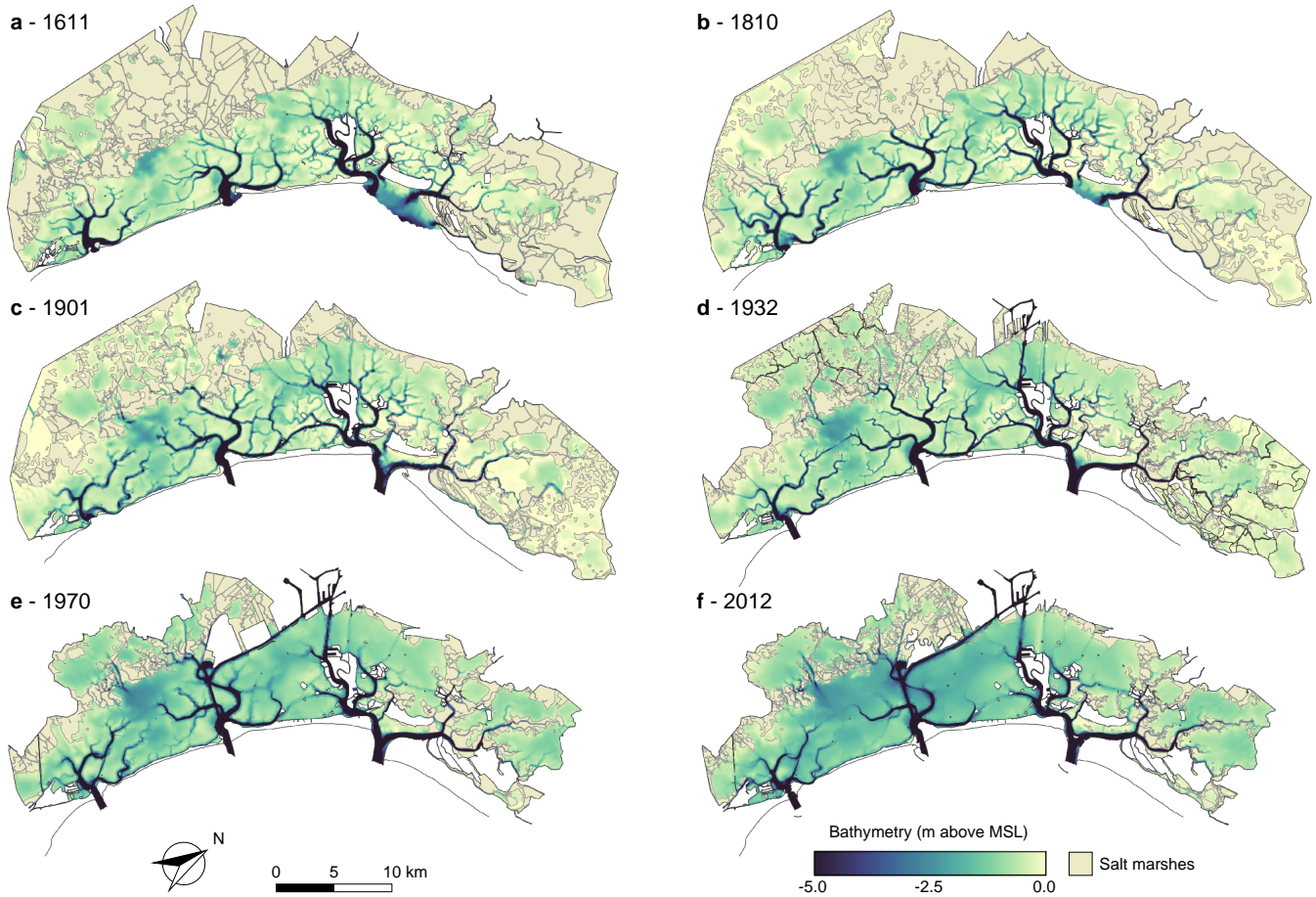


**Figure 1. Historical bathymetries of the Venice Lagoon.** Color-coded bathymetries of the six different configurations of the Venice Lagoon: 1611 (a), 1810 (b), 1901 (c), 1932 (d), 1970 (e), and 2012 (f).

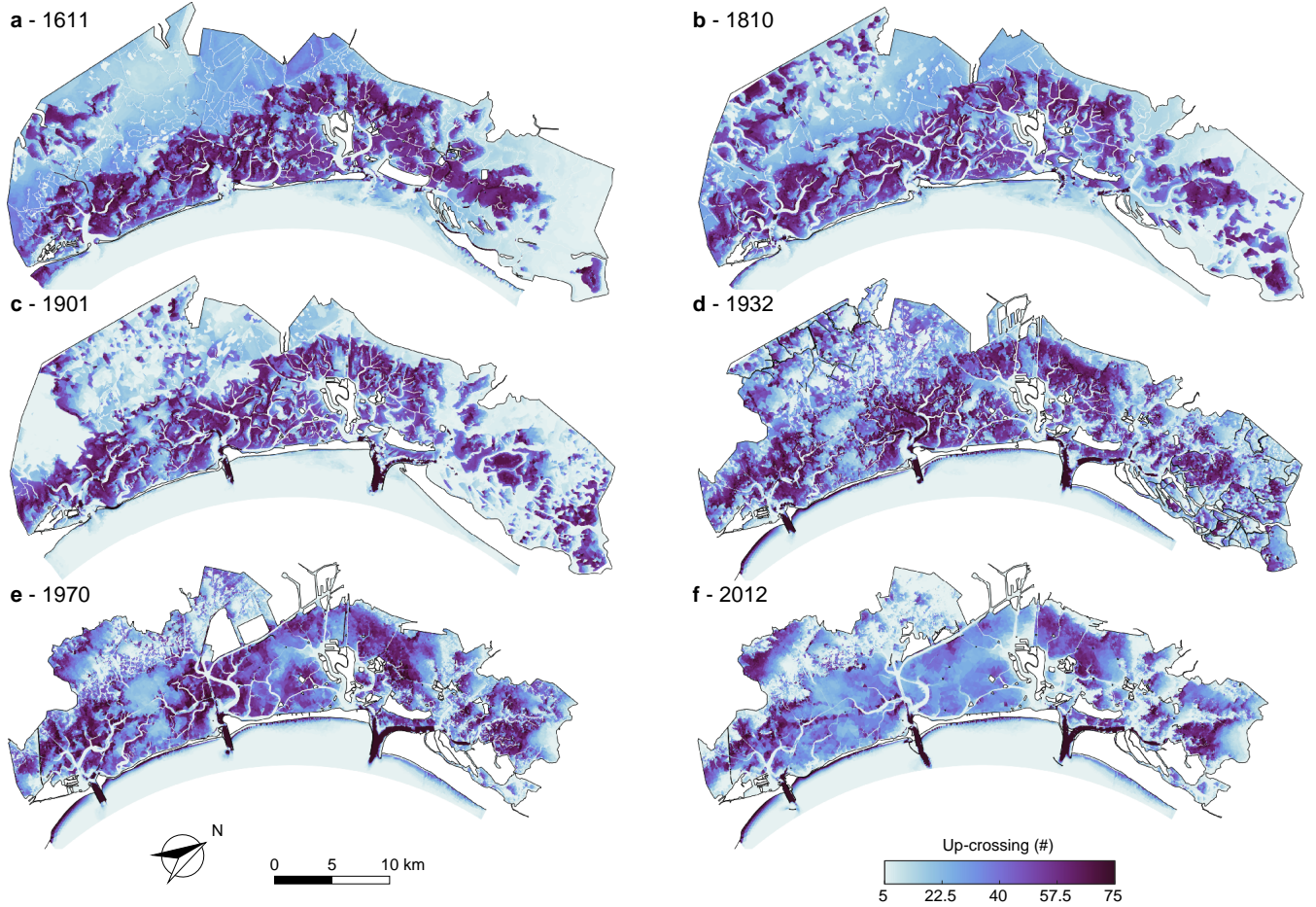


**Figure 2. Number of upcrossings of the erosion threshold.** Spatial distribution of the number of upcrossings of the threshold for erosion  $\tau_c = 0.4$  Pa for the six different configurations of the Venice Lagoon: 1611 (a), 1810 (b), 1901 (c), 1932 (d), 1970 (e), and 2012 (f).



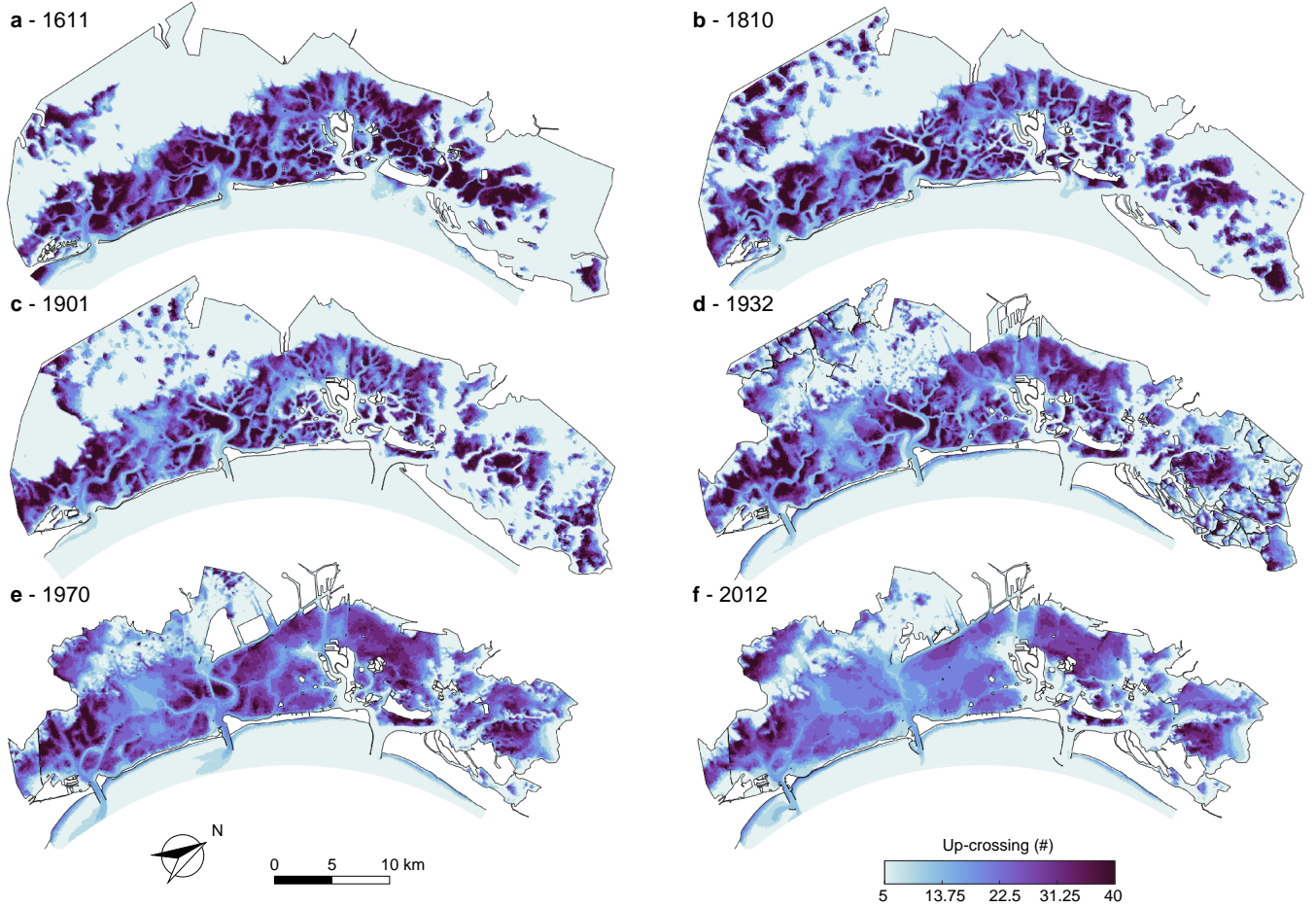


**Figure 3. Number of upcrossings of the SSC threshold.** Spatial distribution of the number of upcrossing of the threshold for suspended sediment concentration  $C_0 = 40 \text{ mg l}^{-1}$ , for the six different configurations of the Venice Lagoon: 1611 (a), 1810 (b), 1901 (c), 1932 (d), 1970 (e), and 2012 (f).



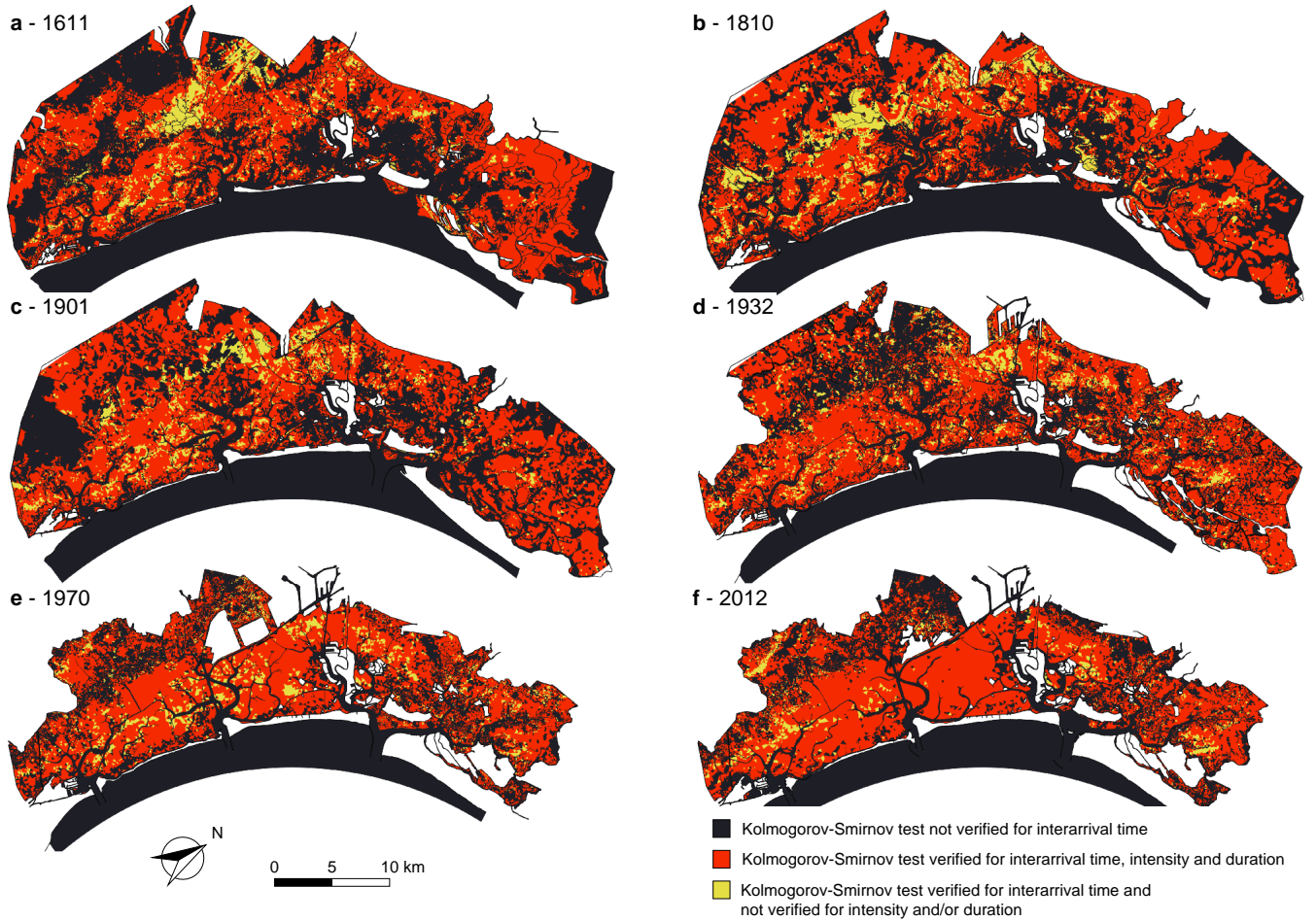
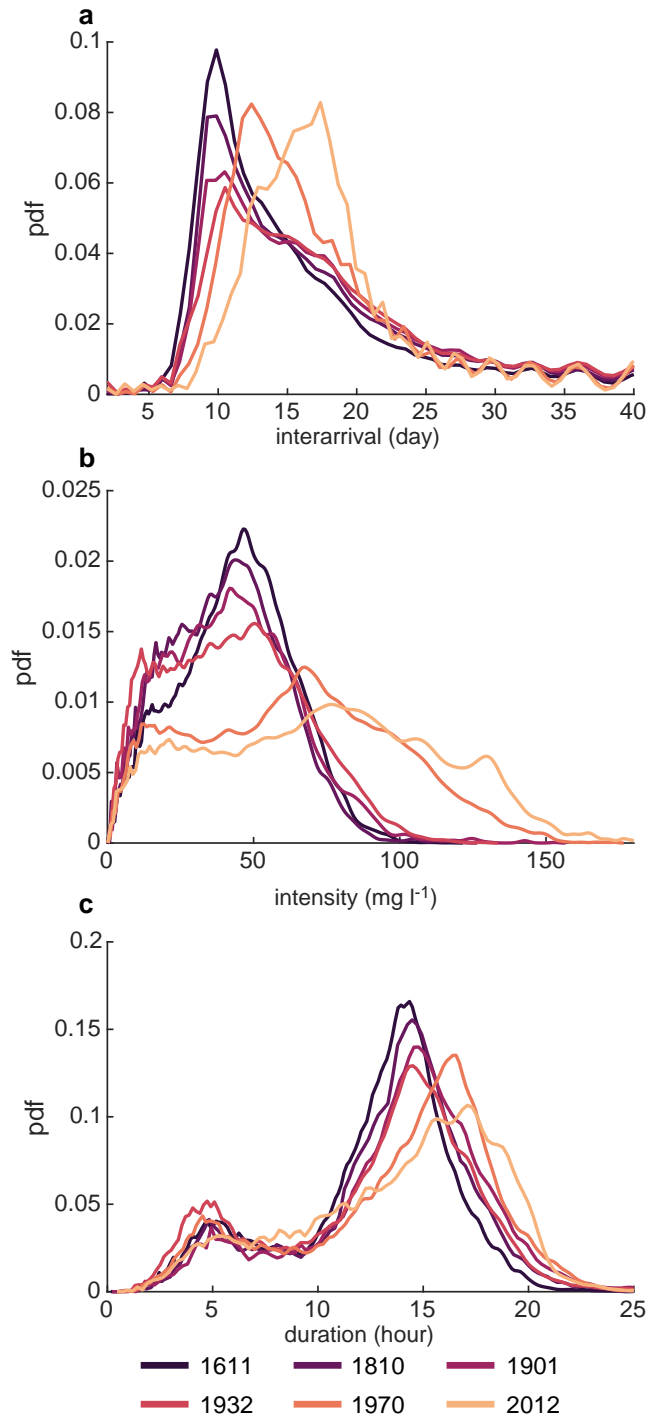


**Figure 4. Kolmogorov-Smirnov test for over-threshold erosion events.** Spatial distribution of Kolmogorov-Smirnov (KS) test at significance level ( $\alpha = 0.05$ ) for the six different configurations of the Venice Lagoon: 1611 (a), 1810 (b), 1901 (c), 1932 (d), 1970 (e), and 2012 (f). In the maps we can distinguish areas where the KS test is: not verified (dark blue); verified for all the considered stochastic variables (interarrival time, intensity over-the threshold and duration) (red); verified for the interarrival time and not for intensity and/or duration (yellow).



Year	$t$ [day]	
	(mean $\pm$ std)	(median)
1611	27.49 $\pm$ 36.45	14.96
1810	29.35 $\pm$ 36.32	16.47
1901	32.47 $\pm$ 40.30	17.93
1932	33.59 $\pm$ 41.09	18.31
1970	27.87 $\pm$ 32.87	16.47
2012	29.24 $\pm$ 32.25	17.95

Year	$e$ [mg l <sup>-1</sup> ]	
	(mean $\pm$ std)	(median)
1611	44.20 $\pm$ 19.00	44.99
1810	40.84 $\pm$ 19.17	41.05
1901	42.66 $\pm$ 21.80	41.96
1932	43.49 $\pm$ 23.36	42.95
1970	64.16 $\pm$ 33.86	65.02
2012	73.21 $\pm$ 38.85	74.68

Year	$d$ [hour]	
	(mean $\pm$ std)	(median)
1611	12.58 $\pm$ 3.91	13.50
1810	13.23 $\pm$ 4.12	14.02
1901	13.78 $\pm$ 4.27	14.46
1932	12.71 $\pm$ 4.71	13.85
1970	13.76 $\pm$ 4.73	14.98
2012	13.96 $\pm$ 4.70	14.96

**Figure 5. Spatial probability density function of interarrival time, intensity and duration of SSC over-threshold events.** Probability density function (left), mean (mean  $\pm$  standard deviation) and median value (right) of interarrival times  $t$  (a), intensity  $e$  (b) and duration  $d$  (c) of SSC over-threshold events.

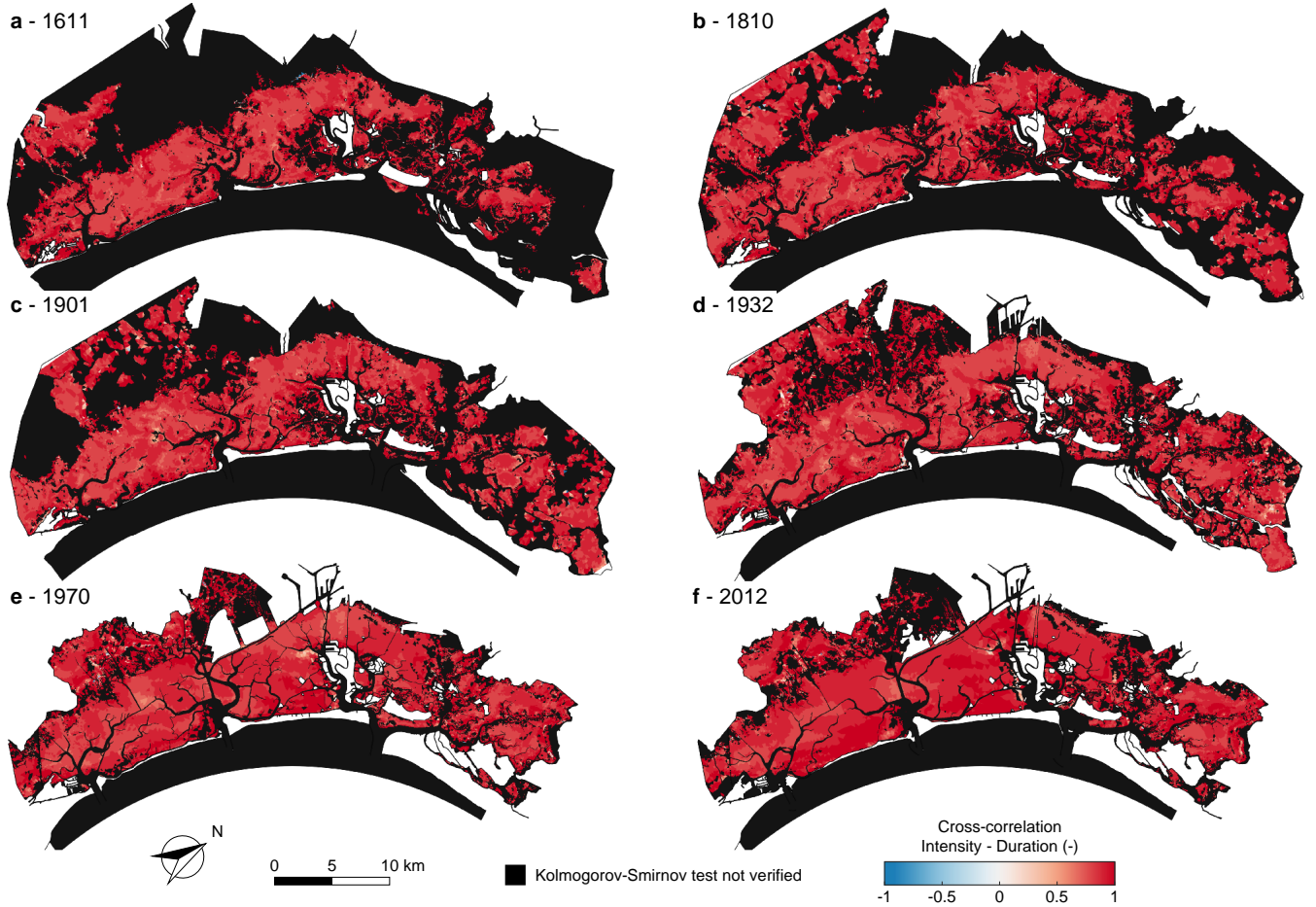


**Figure 6. Cross-correlation between intensity and duration over-threshold SSC events.** Spatial distribution of temporal cross-correlation between intensity of peak-excesses and duration of over-threshold exceedances for the six different configurations of the Venice Lagoon: 1611 (a), 1810 (b), 1901 (c), 1932 (d), 1970 (e), and 2012 (f). Black identifies sites where over-threshold SSC events cannot be modeled as a marked Poisson process (i.e. the KS test is not verified for the interarrival time).

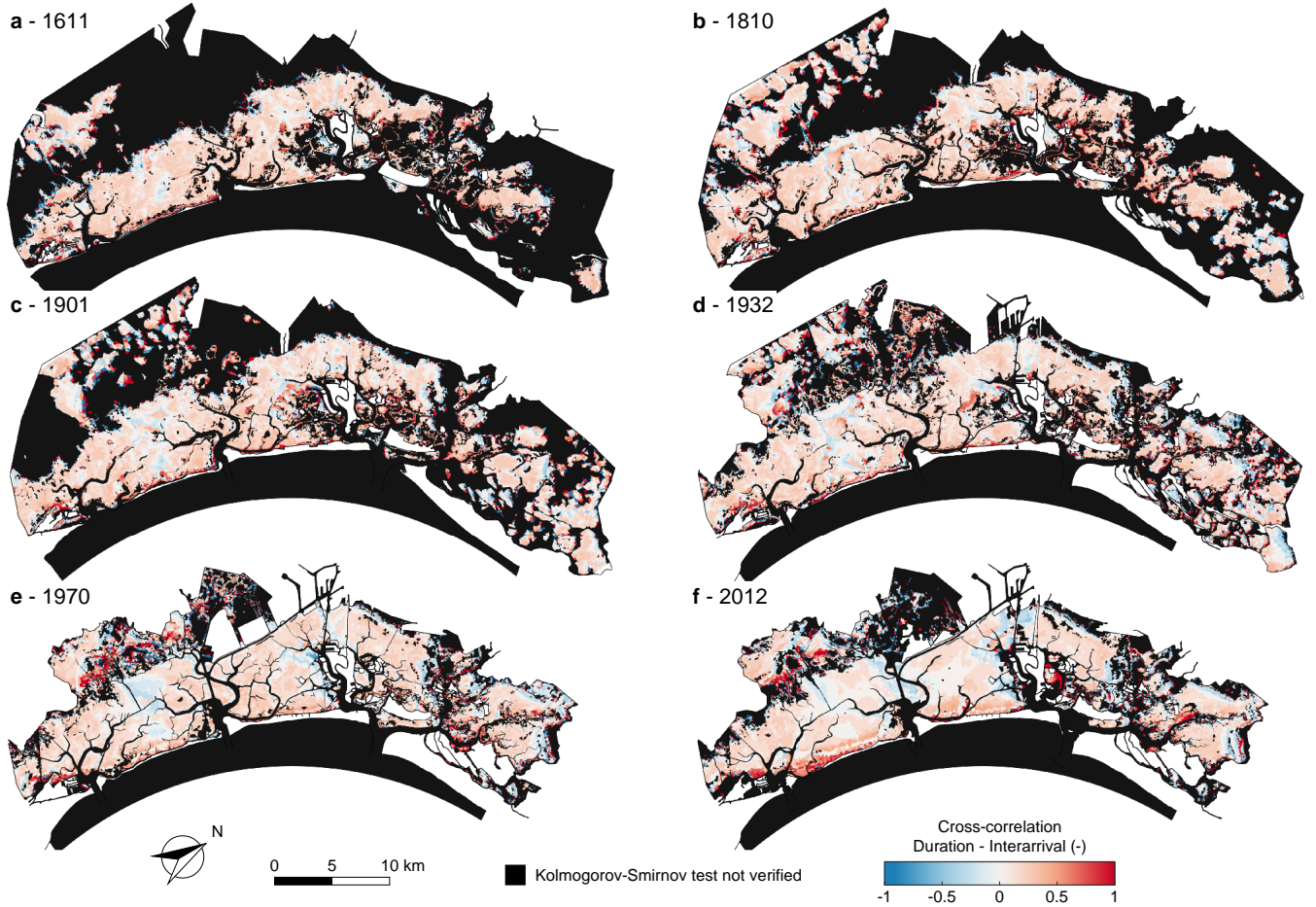


**Figure 7. Cross-correlation between duration and interarrival times over-threshold SSC events.** Spatial distribution of temporal cross-correlation between duration and interarrival times of over-threshold exceedances for the six different configurations of the Venice Lagoon: 1611 (a), 1810 (b), 1901 (c), 1932 (d), 1970 (e), and 2012 (f). Black identifies sites where over-threshold SSC events cannot be modeled as a marked Poisson process (i.e. the KS test is not verified for the interarrival time).



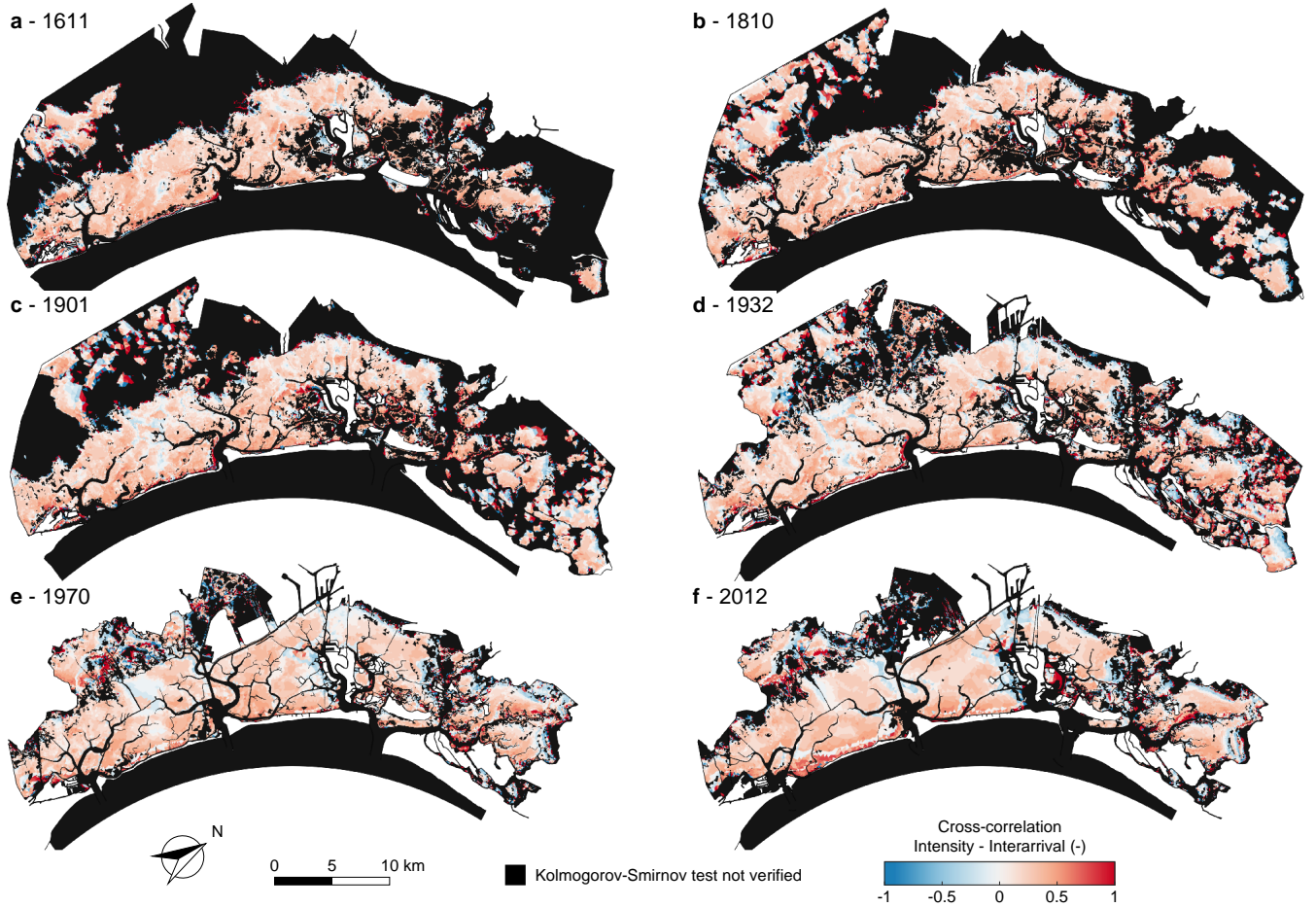


**Figure 8. Cross-correlation between intensity and interarrival times of over-threshold SSC events.** Spatial distribution of temporal cross-correlation between intensity of peak-excesses and interarrival times of over-threshold exceedances for the six different configurations of the Venice Lagoon: 1611 (a), 1810 (b), 1901 (c), 1932 (d), 1970 (e), and 2012 (f). Black identifies sites where over-threshold SSC events cannot be modeled as a marked Poisson process (i.e. the KS test is not verified for the interarrival time).

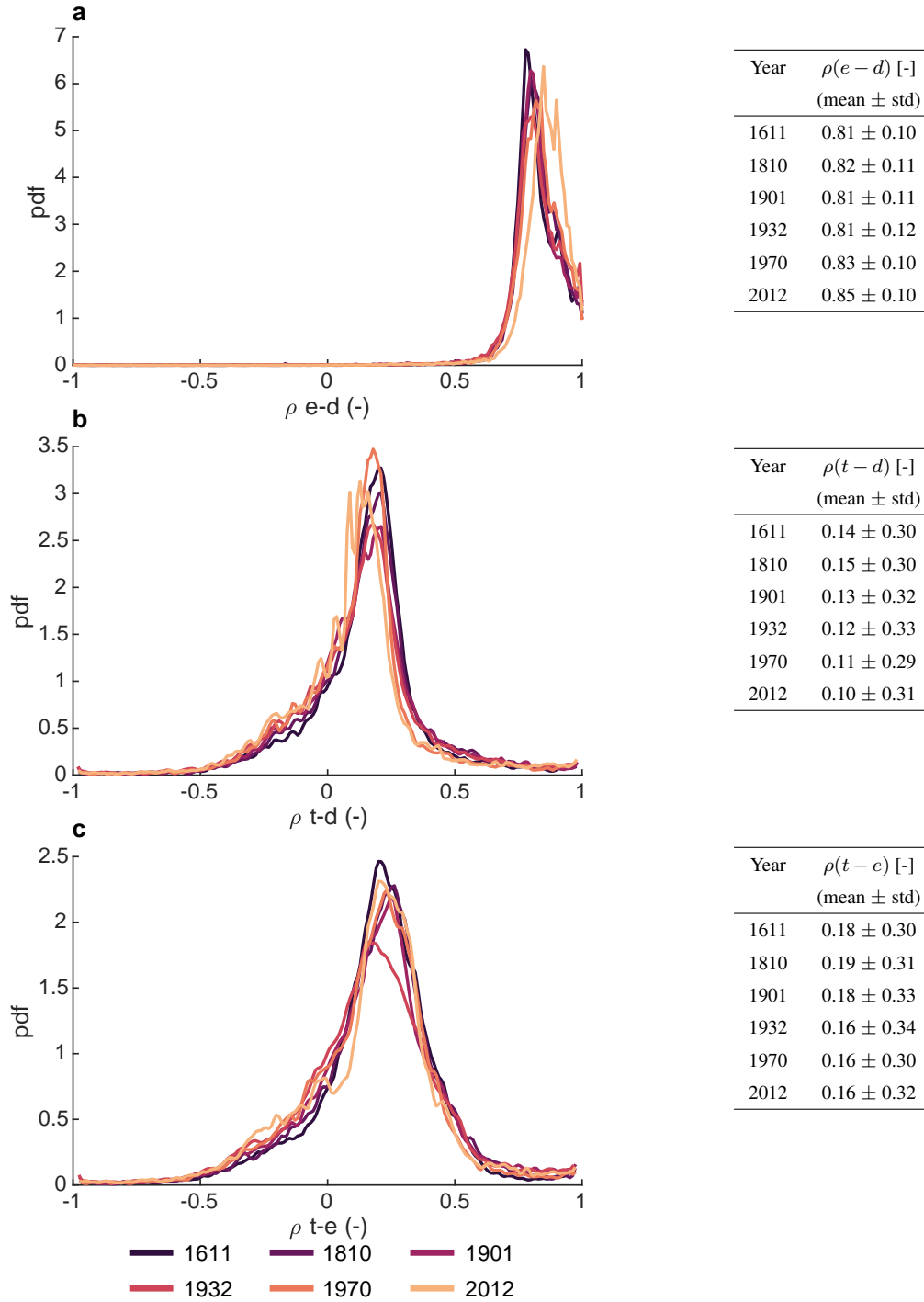


**Figure 9. Spatial probability density function of cross-correlation between interarrival time, intensity and duration of SSC over-threshold events.** Probability density function (left) and mean value (mean  $\pm$  standard deviation, right) of cross-correlation between intensity and duration  $\rho(e-d)$  (a), interarrival time and duration  $\rho(t-d)$  (b) and interarrival time and intensity  $\rho(t-e)$  (c).